Maneuverability, State of the art

Prof. Dr S. Motora / University of Tokyo, Department of Naval Architecture, Tokyo

Introduction

Up to the early 1940s, most studies in the field of ship maneuverability had been focused on the turning qualities, and the work of Hovgard [1] can be taken as a good example. Very little work had been published on course keeping qualities, but among them the work of Weinblum [2] is surprisingly advanced. However, it was not successful in drawing public attention towards this important topic.
The work of Davidson and Schiff in 1944 and 1946 [3, 4] presented new approaches to the problem, and in about the same period, Kempf's standard maneuver [5] and Dieudonné's spiral test [6] were introduced which, together with Davidson's work, opened a new age of studying ship maneuverability by considering the course keeping qualities and transient response.
There has also been remarkable progress in the field of model experiment techniques. Together with the rotating arm technique, the planar motion mechanism technique, which was introduced by Gertler [10, 11] in testing submarines, has become common for testing surface ships. Measuring techniques using radio controlled free running models have also developed rapidly, and have become quite common.
Nomoto's work [8, 9] on frequency response analysis and the first order simulation of ship maneuverability which was developed from the analysis of Kempf's standard maneuver, have given a clear explanation of the relationship between the course keeping quality and the turning ability, and gave impetus to the development of the method of treating ship maneuverability as an open loop system responding to the helm angle.
In accordance with the rapid development of computers, the application of computers to the simulation of ship motion has been developed in recent years in two ways. First, simulation for training purposes, mainly based on analogue computers, and secondly the calculation and prediction of maneuvering motions, mainly based on digital computers.
Recently, further attempts are being made to treat ship maneuverability as a 'closed loop system' since the ship's response is always fed back through a control system which may be either a human or auto-pilot system.
At the first symposium on maneuverability of ships at DTMB in 1960, Norrbin [12] made a broad survey of the development of studies in this field. In this paper, the author will attempt to review the progress in this field since 1960.

Equations of motion

Derivation of the equation of motion

In early studies, the equation of motion was constructed using a co-ordinate system in which the direction of ship's speed was taken as a main axis; this method has been used in aeronautics. Davidson and Schiff's papers [3, 4] in 1944 and 1946 were the first to introduce a co-ordinate system based on a body-fixed axis. Since then, this method of choosing co-ordinates has become common because in this way the hydrodynamic coefficients are easier to obtain and the equation of motion is simplified [13]. If we take the co-ordinate system as shown in Fig. 1, the equation of motion is written as follows (for the notations reference is made to the list of symbols at the end of this paper):

$$\left.\begin{aligned} m(\dot{u} - vr) &= X \\ m(\dot{v} + ur) &= Y \\ I_z\dot{r} &= N \end{aligned}\right\} \qquad (1)$$

where the right hand side represents the hydrodynamic forces and moments which are functions of acceleration, velocity, and helm angle etc.

Linear equation

There are two ways of linearizing equation (1). One is based on an elegant equation of motion for a solid passing through an ideal fluid given by Lamb [15] in which the added mass and added moment of inertia are emphasized. Davidson [4], and Motora [14] have used this type of equation. The other is to expand the hydrodynamic force and moment by the Taylor expansion and

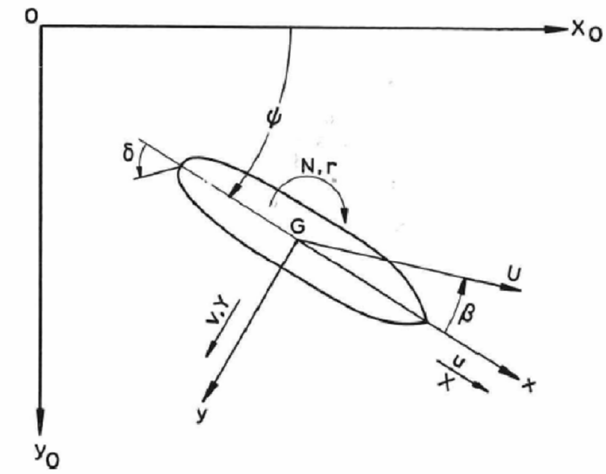

Fig. 1

to pick out the first order terms. In this way, the added mass is treated only as an acceleration derivative. Abkowitz [16] has used this type of equation followed by Norrbin [12] and others. Using the first method, the equation of motion will be written as follows:

$$\begin{aligned}&(m + m_y)\dot{v} + x_x m_y \dot{r} = Y_v v + \\ &+ \{-(m + m_x)u + Y_r{}^*\}\, r + Y_{\dot{\delta}}\dot{\delta} + Y_\delta \delta \\ &(I_z + J_z)\dot{r} + \dot{\alpha}_x m_y \dot{v} = N_v v + N_r r + N_{\dot{\delta}}\dot{\delta} + N_\delta \delta\end{aligned} \tag{2}$$

where the terms for the x direction have been omitted. Using the second method, the equation takes the following form:

$$\left.\begin{aligned}&(m - Y_{\dot{v}})\dot{v} - Y_{\dot{r}}\dot{r} = Y_v v + (-mu + Y_r)r + \\ &+ Y_{\dot{\delta}}\dot{\delta} + Y_\delta \delta \\ &(I_z - J_z)\dot{r} - N_{\dot{v}}\dot{v} = N_v v + N_r r + N_{\dot{\delta}}\dot{\delta} + N_\delta \delta\end{aligned}\right\} \tag{3}$$

Usually equations (2) and (3) are normalized and the variable v is converted into β by the following expression:

$$\left.\begin{aligned}&(m' - Y_{\dot{v}}')\dot{\beta}' - Y_{\dot{r}}'\dot{r}' = Y_\beta'\beta' + (-m' + Y'_r)r' + \\ &+ Y_{\dot{\delta}}'\dot{\delta}' + Y'_\delta\delta' \\ &(I'_z - N_{\dot{r}}')\dot{r}' - N_{\dot{\beta}}'\dot{\beta}' = N_\beta'\beta' + N'_r r' + \\ &+ N'_{\dot{\delta}}\dot{\delta}' + N'_\delta\delta'\end{aligned}\right\} \tag{4}$$

where ′ (prime) indicates that the quantity is normalized. (see list of symbols).

For practical calculations, the β in equation (4) is usually eliminated and the equation is converted into second order equation of r for which Nomoto's expression [7] is the most common.

$$T'_1 T'_2 \ddot{r}' + (T'_1 + T'_2)\dot{r}' + r' = K'\delta' + K'T'_3\dot{\delta}' \tag{5}$$

where:

$$\begin{aligned}&T'_1 T'_2 = \{(Y_{\dot{v}}' - m')(N'_{\dot{r}} - I'_z) - N'_{\dot{v}}Y'_{\dot{r}}\}/D \\ &T'_1 + T'_2 = [\{(Y'_{\dot{v}} - m')N'_r + (N_{\dot{r}} - I'_z)Y'_v\} - \\ &- \{Y'_{\dot{v}}N'_v + N'_{\dot{v}}(Y'_r - m')\}]/D \\ &K' = N'_v Y'_\delta - Y'_v N'_\delta)/D \\ &K'T'_3 \quad = \{N'_{\dot{v}}Y'_\delta - (Y'_{\dot{v}} - m)N'_\delta\}/D \\ &D \quad = Y'_v N'_r - N'_v(Y'_r - m')\end{aligned} \tag{6}$$

where D is the determinant for the course stability, and $K'\,\delta' = L/R$ corresponds to a non-dimensionalized steady turning velocity. By this expression, a transfer function of ship response to helm angle is neatly obtained by automation theory as follows:

$$Y'(p) = \frac{K'(1 + T'_3 p)}{(1 + T_1' p)(1 + T'_2 p)} \tag{7}$$

Non-linear equations

In the case of directionally stable ships, linear equations give fairly good results at low turning velocities. However, in case of directionally unstable ships or marginally stable ships such as supertankers, linear equations do not give good agreement with full scale data even at low angular velocities. In recent years, non-linear equations have been used in these cases. In dealing with non-linear equations, there are two approaches. One is to add the minimum number of non-linear terms to a linear equation in order to obtain a sufficiently good approximation for a specified purpose. In this case, because the number of non-linear terms is small, it is possible to express the non-linearity by a small number of parameters. This method is suitable for use in defining the maneuverability with a small number of parameters. The second approach is to add many higher order derivatives in order to get as accurate a result as possible. This method is mainly used for the simulation or prediction of motions, and is commonly used with digital computers.

a When an r^3 term is added as a non-linear term. Norrbin [91], Nomoto [17], van Leeuwen [18] and Glansdorp [20] have suggested adding an r^3 term to the linear equation as follows:

$$\begin{aligned}&T'_1 T'_2 \ddot{r}' + (T'_1 + T'_2)\dot{r}' + r' + ar'^3 = \\ &= K'\delta' + K'T'_3\dot{\delta}'\end{aligned} \tag{8}$$

where the coefficient α is chosen so that when $\ddot{r}$, $\dot{r}$ and $\dot{\delta}$ are put zero eq. (8) gives the best fit to a $\delta - r$ curve obtained from a spiral test. The most attractive feature of this method is that it is possible to express the non-linearity by only one parameter α.

Van Leeuwen [18] suggested a similar expression for the equation in the x direction as follows:

$$T_u \dot{u} + u = K_u \cdot r^2$$

b Adding a non-linear term to give more accurate simulation of spiral test results.

Bech, Smitt [21] and Norrbin [19] proposed a method in which the turning velocity r in a steady turning state is exactly given by a spiral test result; viz. instead of the r' term of eq. (5), $K'H(r')$ is substituted:

$$\ddot{r}' + \left(\frac{1}{T'_1} + \frac{1}{T'_2}\right)\dot{r}' + \frac{K'}{T'_1 T'_2} H(r') = \frac{K'}{T'_1 T'_2} (T_3' \dot{\delta}' + \delta') \tag{9}$$

where $H(r') = \delta'$ is the relationship between the steady r' and δ' obtained by a spiral test. At a steady state, since $\ddot{r}' = \dot{r}_r = \dot{\delta}' = 0$, we get

$$H(r') = \delta'$$

Thus, the simulation of motion at a steady state is perfect. (see Fig. 2) In the course of deriving eq. (9), Bech and Smitt [21] have shown that $(1/T'_1 + 1/T'_2)$ and $K'/T_1 T'_2$ stay fairly constant in any stage of motion provided the advance speed is unchanged. Therefore, it is expected that eq. (9) will give a fairly accurate approximation of the motion for the transient stage of steered motion. Norrbin [19] has suggested that instead of $H(r') = \delta'$, $\dot{\Psi}' - \alpha \mid \dot{\Psi}'^n \mid \dot{\Psi}' = \delta'$ may be used.

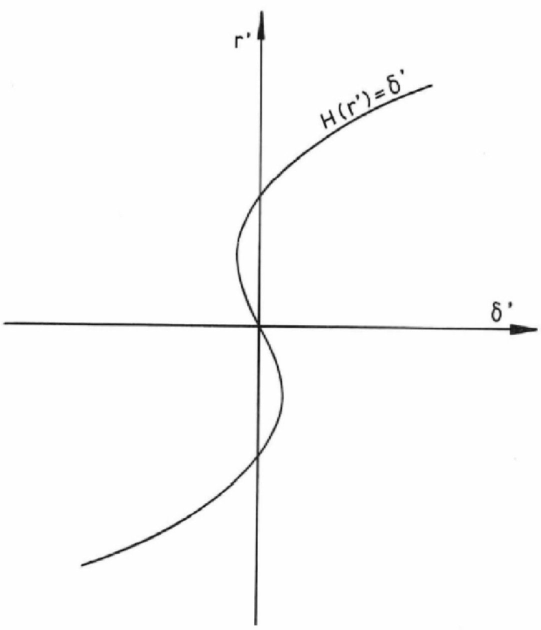

Fig. 2

Simulation by higher order equations

As digital computers become more available, several trials have been made to simulate ship motions by higher order equations. This method is not suitable to express the maneuverability by a small number of parameters as in a and b, but it is suitable to predict ship motions under given conditions. Since it is not practical to cover too many conditions in a full scale test or a model experiment, this method is quite usable for predicting ship motions in any circumstances or in designing auto-pilots. In this method, the right hand side of eq. (1) is expanded into higher order terms. Usually, only even/odd terms are picked up if the hydrodynamic force under consideration is an even/odd function of the variable concerned. As far as a linear equation is concerned, the effect of the advance speed on the maneuverability is very small, so in eq. (2) and (3) the changes in the advance speed have been neglected. However, in the case of higher order non-linear equations, the effect of changes in the speed cannot be neglected anymore. Therefore, we need an equation for the x direction. These equations will take the following form:

$$\left.\begin{aligned} (m - X_{\dot{u}})\dot{u} &= f_1(u, v, r, \delta) \\ (m - Y_{\dot{v}})\dot{v} - Y_{\dot{r}}\dot{r} &= f_2(u, v, r, \delta) \\ - N_{\dot{v}}\dot{v} + (I_z - N_{\dot{r}})\dot{r} &= f_3(u, v, r, \delta) \end{aligned}\right\} \tag{10}$$

$$\begin{aligned} f_1(u, v, r, \delta) = {} & X^0 + X_u \Delta u + \tfrac{1}{2} X_{uu} \Delta u^2 + \tfrac{1}{6} X_{uuu} \Delta u^3 \\ & + \tfrac{1}{2} X_{vv} v^2 + \tfrac{1}{2} X_{rr} r^2 + \tfrac{1}{2} X_{\delta\delta} \delta^2 \\ & + \tfrac{1}{2} X_{vvu} v^2 \Delta u + \tfrac{1}{2} X_{rru} r^2 \Delta u + \tfrac{1}{2} X_{\delta\delta u} \delta^2 \Delta u \\ & + (X_{vr} + m) vr + X_{v\delta} v\delta + X_{r\delta} r\delta + X_{vru} vr \Delta u \\ & + X_{v\delta u} v\delta \Delta u + X_{r\delta u} r\delta \Delta u \end{aligned}$$

$$\begin{aligned} f_2(u, v, r, \delta) = {} & Y^0 + Y^0{}_u \Delta u + Y^0{}_{uu} \Delta u^2 + Y_v v \\ & + \tfrac{1}{6} Y_{vvv} v^3 + \tfrac{1}{2} Y_{vrr} v r^2 + \tfrac{1}{2} Y_{v\delta\delta} v \delta^2 + Y_{vu} v \Delta u \\ & + \tfrac{1}{2} Y_{vuu} v \Delta u^2 + (Y_r - m u_1)\, r + \tfrac{1}{6} Y_{rrr} r^3 + \tfrac{1}{2} Y_{rvv} r v^2 \\ & + \tfrac{1}{2} Y_{r\delta\delta} r \delta^2 + Y_{ru} r \Delta u + \tfrac{1}{2} Y_{ruu} r \Delta u^2 + Y_\delta \delta \\ & + \tfrac{1}{6} Y_{\delta\delta\delta} \delta^3 + \tfrac{1}{2} Y_{\delta vv} \delta v^2 + \tfrac{1}{2} Y_{\delta rr} \delta r^2 \\ & + Y_{\delta u} \delta \Delta u + \tfrac{1}{2} Y_{\delta uu} \delta \Delta u^2 + Y_{vr\delta} v r \delta \end{aligned}$$

$$\begin{aligned} f_3(u, v, r, \delta) = {} & (\, N^0 + N^0{}_u \Delta u + N^0{}_{uu} \Delta u^2 + N_v v \\ & + \tfrac{1}{6} N_{vvv} v^3 + \tfrac{1}{2} N_{vrr} v r^2 + \tfrac{1}{2} N_{v\delta\delta} v \delta^2 + N_{vu} v \Delta u \\ & + \tfrac{1}{2} N_{vuu} v \Delta u^2 + N_r r + \tfrac{1}{6} N_{rrr} r^3 \\ & + \tfrac{1}{2} N_{rvv} r v^2 + \tfrac{1}{2} N_{r\delta\delta} r \delta^2 + N_{ru} r \Delta u + \tfrac{1}{2} N_{ruu} r \Delta u^2 \\ & + N_\delta \delta + \tfrac{1}{6} N_{\delta\delta\delta} \delta^3 + \tfrac{1}{2} N_{\delta vv} \delta v^2 + \tfrac{1}{2} N_{\delta rr} \delta r^2 \\ & + N_{\delta u} \delta \Delta u + \tfrac{1}{2} N_{\delta uu} \delta \Delta u^2 + N_{vr\delta} v r \delta \end{aligned}$$

where, for instance, Y_{rvv} indicates $\dfrac{\partial^3 Y}{\partial r \cdot \partial v^2}$. The relative contribution of higher order terms to the computed results has been examined by Strøm-Tejsen [22], and Eda and Crane [23]. In practice, only those terms which make significant contributions to the results are picked up into the equations.

Recently, Clarke [24] tried to substitute steady state values of r and v into the non-linear terms instead of the transient values of r and v and thus to simplify the equation in the same style as the linear equation (5) as follows:

$$\begin{aligned} &A_0 \ddot{r}' + (A_1 + A_2 r' + A_3 r'^2)\dot{r}' + \\ &+ (A_4 + A_5 r' + A_6 r'^4)\, r' + (A_7 + A_8 \delta'^2)\, \dot{\delta}' + \\ &+ (A_9 + A_{10}\delta'^2)\, \delta' + A_{11} = 0 \end{aligned} \quad (11)$$

where $A_0 \sim A_{11}$ are constants depending on the ship. Comparing eq. (11) with eq. (8), it will be noticed that the coefficient of r' in eq. (8) is also a non-linear function of $\dot{r}'$ in eq. (11). According to Clarke, the effect of using the steady state value of r and v for the non-linear terms is naturally zero for the steady state results and is very slight for transient state results. In Fig. 3, the difference between results obtained from eq. (10) and eq. (11) is shown by a phase-plane portrait ($\dot{r} - r$ diagram).

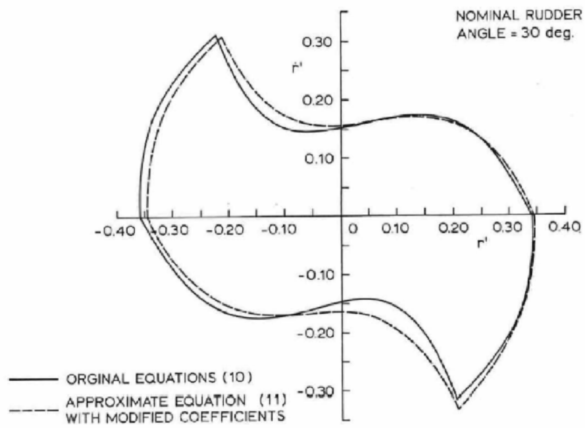

Fig. 3 $\dot{r}' - r'$ phase portrait for = 30 deg. Kempf maneuver (modified A_2 and A_3).

Derivatives

Effect of frequency

As the hydrodynamic force and moment induced by ship motion are affected by the presence of a free surface, derivatives in the equations of motion should be functions of frequency. For the acceleration derivative $Y_{\dot{v}}$ and the sway damping derivative Y_v for a two-dimensional body, theoretical calculations have been made by Grim [25], Tasai [27], Tamura [26] and Porter [28]. It is also ascertained by model experiments that these derivatives are frequency dependent. In Fig. 4 experimental [30] and theoretical [29] values of $Y_{\dot{v}}$ and $N_{\dot{v}}$ for a Series 60 0.70 block model are shown. (referred from [31]). Since

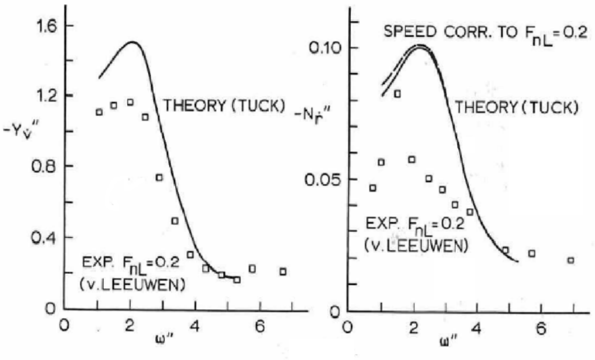

Fig. 4 Total added mass and added moment of inertia for a series 60 Block .70 form according to theory and experiments.

steering motions, except steady turns, are composed of sinusoidal motions of many frequencies, high accuracy is required when making the derivatives functions of frequency. However, most of the derivatives have not yet been obtained as functions of frequency, and we are obliged to adopt a constant value for each derivative, corresponding to a specified frequency which seems to be a representative value of the frequencies involved in the motion under consideration.

The next question is which frequency should be taken as representative. In the case of zig-zag maneuvers or similar kinds of steering motions which are often used in keeping the ship's heading, the average frequency is quite low. Therefore we may choose the representative frequency as zero. However, in case of a collision or the response of ships to stepwise changes in the helm angle, a higher frequency component may be included. Motora, Fujino and others [32] have made some observations on this problem. They computed an exact sway velocity v due to a stepwise input of helm angle of duration τ making use of the frequency dependent $Y_{\dot{v}}$ and Y_v. They then obtained an equivalent added mass $\overline{Y}_{\dot{v}}$ which is a constant independent of time and will give the same v when the time elapsed is τ. This equivalent added mass thus obtained is as shown in Fig. 5 together with experimental data. From Fig. 5, we know that if τ is longer than a few seconds in full scale time, the equivalent added mass is practically the same value as $Y_{\dot{v}}$ at zero frequency.

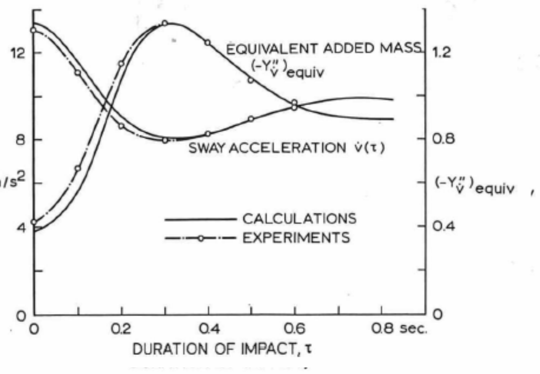

Fig. 5 Equivalent added mass coefficient as defined by acceleration due to step input impact of duration τ.

Therefore, we may conclude that for ordinary steering motions, we can use the value of $Y_{\dot{v}}$ at zero frequency as a representative value even in cases when the rudder is moved frequently. While there has been no similar study other than acceleration derivatives, Brard [34] suggested a method of examining the effect of frequency on the damping derivatives. Newman [35] pointed out that since the frequency parameter for viscosity is $\omega L/V$ and the frequency parameter for the free surface effect is $\omega V/g$ there will be no frequency effect when both parameters are negligible, and that the effect of frequency upon the viscosity will appear before the free surface phenomena are affected. According to Newman, the critical frequency at which the damping derivatives begin to be affected will be something like a 20°–20° zig-zag manoeuvre.

Acceleration derivatives

Acceleration derivatives such as $Y_{\dot{v}}$, $Y_{\dot{r}}$, $N_{\dot{v}}$, and $N_{\dot{r}}$ have been used as added mass or added moments of inertia and are mostly obtained by a PMM technique. The rotating arm technique is not suitable in getting acceleration derivatives. An indicial response method has also been tried [33]. Theoretically, $Y_{\dot{v}}''$ for prisms of Lewis form sections have been obtained [25], [26], [27], [29]. Therefore, acceleration derivatives for any ship form can be obtained by making use of the strip method. Comparison of theoretical values with experimental data is shown in Fig. 4. As mentioned in the previous section, acceleration derivatives for zero frequency are used.

Velocity derivatives

There are many studies on velocity derivatives both theoretical and experimental. In the experimental method, the rotating arm technique has long been used until the recent advent of the PMM technique.

The ITTC Maneuverability Committee has conducted a cooperative test program by many world-wide establishments concerning the measurement of the derivatives of Mariner Type ships. In this program, each establishment measured the derivatives by its own conventional test techniques. The following have contributed to the program: Chislet and Strøm-Tejsen [38] making use of the Hya PMM, Paulling using a compact PMM of the University of California [39], van Leeuwen and Glansdorp using the PMM of Delft University [40], Motora and Fujino using the PMM of the University of Tokyo [40], Suarez using the rotating arm of the Davidson Laboratory [42], Gertler using the rotating arm of the NSRDC [37], Kasai using the PMM of Mitsubishi [44], Firsoff using the rotating arm of the Leningrad Institute [41], Burcher using the rotating arm of AEW [43]. Data submitted were collated and analyzed by Gertler [36]. These results are shown in Table 1 together with full scale data by Morse and Price [45] on the 'Compass Island'. Results obtained by the rotating arm and the PMM seem to agree fairly well.

On the theoretical side, the low-aspect ratio wing theory developed by von Kármán and Bolley [47], Jones [48], Weissinger and Lawrence [49] has been applied to obtain hydrodynamic force and moments, acting on a drifting or turning ship, by Thieme [50], Fedyaevsky [53] Jacobs [51] and Inoue [52]. In these theories, the distribution of the bound vortex and direction of the free vortex sheet are properly assumed to give reasonable results. However, since these phenomena are associated by viscosity, the hydrodynamic relation between the vortex distribution and the ship's form has not been thoroughly clarified. Inoue [52] and Fedyaevsky [53] have derived semi-empirical formulae for the hydrodynamic force and moment by introducing some coefficients which are chosen to fit each ship's form. Velocity derivatives obtained by different methods are compared in Table 2. Newman [55] has given a method of calculating derivatives by the slender body theory. The results of his calculation are compared with measured hydrodynamic forces of the forebody and afterbody of a cargo ship using a double model by Norrbin [54], and are shown in Table 3.

Table 1

Organization	type of test	$Y_v' \times 10^3$	$N_v' \times 10^3$	$Y_\delta' \times 10^3$	$N_\delta' \times 10^3$	$Y_r' \times 10^3$	$N_r' \times 10^3$	$Y_{\dot{v}}' \times 10^3$	$N_{\dot{v}}' \times 10^3$	$Y_{\dot{r}}' \times 10^3$	$N_{\dot{r}}' \times 10^3$
Davidson Lab.	R.A. (Rotating arm)	–13.91	–4.40	3.12	–1.58	4.36	–2.97	–	–	–	–
NSRDC	O.T. (obligue tow)	–16.90	–4.47	2.98	–1.43	–	–	–	–	–	–
	R.A.	–16.90	–4.47	2.87	–1.38	2.62	–2.30	–	–	–	–
Kryloff Inst.	O.T.	–14.9	–3.50	2.69	–1.26	–	–	–	–	–	–
	R.A.	–	–	–	–	1.90	–2.90	–	–	–	–
AEW	R.A.	–14.3	–3.20	2.62	–1.69	2.71	–2.01	–	–	–	–
Paris Basin	R.A.	–15.13	–3.05	2.94	–1.37	3.72	–2.54	–	–	–	–
	R.A.	–12.77	–3.83	2.92	–1.33	3.09	–2.27	–	–	–	–
HyA	O.T.	–11.60	–2.91	2.78	–1.33	–	–	–	–	–	–
	PMM	–	–	–	–	2.72	–1.91	–7.48	–0.13	–0.27	–0.44
TH Delft	O.T.	–11.76	–3.17	2.32	–1.10	–	–	–	–	–	–
	PMM	–10.10	–3.49	–	–	2.90	–2.00	–7.34	–0.19	–0.33	–0.48
Univ. of	O.T.	–9.70	–3.80	–	–	–	–	–	–	–	–
California	PMM	–10.00	–3.80	–	–	2.30	–2.10	–6.70	–0.30	–0.30	–0.40
Techn. Inst.	O.T.	–13.2	–3.72	3.99	–1.46	–	–	–	–	–	–
Mitsubishi	PMM	–	–	–	–	3.33	–1.93	–5.62	–	–	–0.23
Univ. of	O.T.	–14.6	–3.99	2.70	–1.23	–	–	–	–	–	–
Tokyo	PMM	–13.90	–3.96	–	–	2.96	–2.15	–7.12	–0.17	–0.17	–0.40
Full scale ship (Compass Island)		–16.00	–2.80	1.20	–0.60	2.20	–0.98	–	–	–	–
Theory (Jacobs)	without propeller	–14.16	–3.06	–	–	2.96	–2.64	–	–	–	–

Figures were taken from ref. [36 and 37] and [46].
Ship speed is ranging 14 ~ 15 kn except for NSRDC (18 ~ 22 kn), AEW (10 kn) and Mitsubishi (7 ~ 14 kn).

Table 2 Experimental and theoretical values of stability derivatives of Series 60 0.60 block model (From [175])

Derivative	*Experiment*		*Theory*			
	Suarez	*Paul-ling*	*Jacobs*	*Inoue*		*Thieme*
				$K_1=1$	$K_1=0.8$	
$Y'_v \times 10^{+3}$	11.2	12.3	14.2	13.5	10.8	6.77
$N'_v \times 10^{+3}$	3.33	4.00	3.06	4.18	4.18	3.39
$Y'_r \times 10^{+3}$	3.90	2.90	2.96	5.10	4.08	3.39
$N'_r \times 10^{+3}$	1.88	2.20	2.64	2.23	2.23	0.835

Table 3

Method	Y'_β
Low aspect wing theory	0.184
Slender body theory, forebody	0.193
Experiment, forebody	0.203
Experiment, total hull without rudder	0.172
Experiment, total hull with rudder	0.232

Higher order derivatives

As described in the previous section, a theoretical method to obtain derivatives is being developed. Though theoretical derivatives contain a non-linear term due to cross flow, the theory is not yet fully enough developed to be able to give higher order derivatives containing non-linear parts. Therefore, at present, higher order derivatives for simulation purposes are obtained by rotating arm tests or PMM tests. In the case of rotating arm tests, hydrodynamic forces are measured for various combinations of r and β, and higher order derivatives are obtained by a curve fitting method. (for instance see [23]). In the case of PMM tests, measured hydrodynamic forces on a time basis are resolved by Fourier analysis [38, 40]. Results obtained by PMM [38, 40] seem to agree with the results of rotating arm tests [23].

Rudder force and moment

For rudder force and moment, systematic series model tests have not been conducted since Fisher [56] Bottomley [57] Akazaki [58] Darnell [60] etc. Studies since then seem to be rather focused into interaction between a rudder and a propeller, effect of the wake etc [61, 62, 63]. Okada [62] made an extensive study on interaction of the rudder and ship's body and propeller. In his work, the effect of propeller race and wake on the normal force and longitudinal location of its center such as when the propeller shaft center is not lined up to the rudder center etc. is dealt with. Fujii and Tsuda [63] also obtained the effect of presence of ship hull on the direction of stern flow at a rudder.
In recent years, a rudder is rather deemed a part of a ship and derivatives are measured including rudder force and moment.

Full scale test techniques

Zig-zag test and spiral test

The turning test had for a long time been a common full scale maneuvering test technique until Kempf [5] introduced the zig-zag maneuver in 1943 and Dieudonné [6] introduced the spiral test in 1949. Since then, full scale test techniques to examine course stability and transient state of the ship's response to the rudder have been topics of interest. In accordance with the appearance of many ships with poor course keeping ability such as mammoth tankers, the zig-zag maneuver and spiral test have become quite common practice, and nowadays almost every ship is tested in this way. Since these test techniques are quite common, a detailed explanation will be omitted from this review. The ITTC maneuverability committee has, as its task, made up a standard procedure for these tests, and has published it in its report to the 12th ITTC meeting.

Reversed spiral test

The spiral test is one ingeneous way of examining a ship's course keeping quality. However, in conducting spiral tests on supertankers, it is often felt that it is inconvenient in that it takes too much time to get a steady turning rate as the time constant of these ships is very large. Moreover, the turning rate tends to be affected by wind pressure at small rudder angles. Bech introduced the reversed spiral test in 1966 and it was soon supported by many research workers [64, 65]. In this method, the rudder angle δ which will give a specified turning rate r is measured, while in the conventional spiral test, the steady turning rate r corresponding to a specified δ is measured. In the reversed spiral test, the rudder angle obtained usually varies periodically so that the mean value has to be taken.
The most peculiar feature of this method is that in the case of ships with poor course keeping properties it is possible to get an $r - \delta$ relation for the complete range of rudder angles, while in the case of the regular spiral test, the $r - \delta$ curve forms a hysteresis loop. As shown in Fig. 6, the $r - \delta$ curve on the basis of δ is a partially three valued function and the $r - \delta$ curve on the basis of

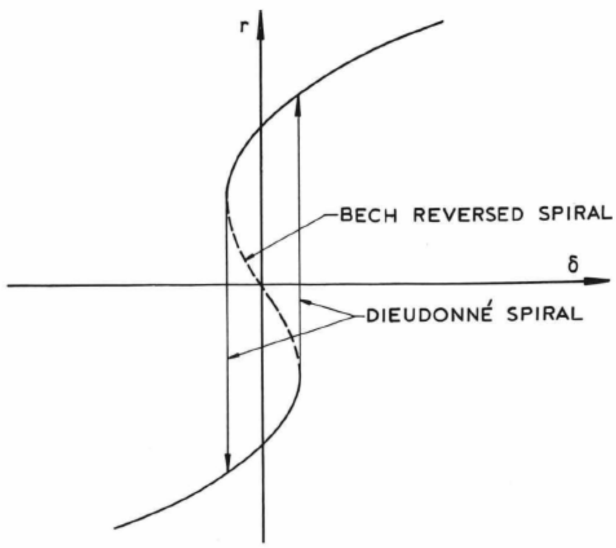

Fig. 6

r is a single valued function. The former corresponds to the regular spiral test and the latter corresponds to the reversed spiral test. The reverse spiral test seems to be suitable for obtaining the ship's characteristics at small rudder angles, particularly for ships with poor course keeping properties.
In practice, it will be convenient to prepare a yaw-rate meter which can show the difference between the pre-set yaw rate and the actual yaw rate. Then a specified yaw rate for which the corresponding rudder angle is required is pre-set on the yaw-rate meter. The helmsman is asked to steer so that the differential yaw rate averages zero. The helm angle thus measured may oscillate, and the average value will give the rudder angle which corresponds to the pre-set yaw rate.
Bech has also tried to use an auto-pilot which can keep the differential yaw rate at zero and obtained satisfactory results.
Stimulated by the zig-zag test and the spiral test, various full scale test techniques have been proposed and are summarized as follows.

Modified zig-zag test

Kempf has proposed a zig-zag maneuver in which the rudder angle was chosen to be 20° and the heading angle at which the rudder is switched was also chosen as 20°. Therefore, ordinary zig-zag tests are run in combinations of equal rudder angle and switching heading angle. (for instance, 10°–10°, 15°–15°, 20°–20° etc.). However, in the case of course unstable ships, the results of zig-zag maneuvers at small rudder angles, say 5°–5°, tend to diverge and will not give steady results.
Thieme and Motora have suggested a modified zig-zag test at which different combinations of rudder angle and the switching heading angle are chosen. (say rudder angle 5° with switching angle 2°, rudder angle 10° with switching angle 5° etc.). The heading angle in this case is chosen smaller than the rudder angle. Thus, it becomes possible to bring the converging motion to a steady state and also makes it possible to keep the yaw rate within a reasonably small range. Motora and Fujino [66] obtained critical combinations of rudder angle and heading angle within which the zig-zag motion will converge. An example is shown in Figs. 7 and 8.
Fig. 7a shows results of a 10°–10° regular zig-zag test and a 5°–1° modified zig-zag test of a ship of which the result of a spiral test is shown in Fig 7b. Since the zig-zag maneuver is treated as the response of a ship to a steering with hysteresis loop as shown in Fig. 8(a), critical combination of switching angle ψ^* and rudder angle δ^* is

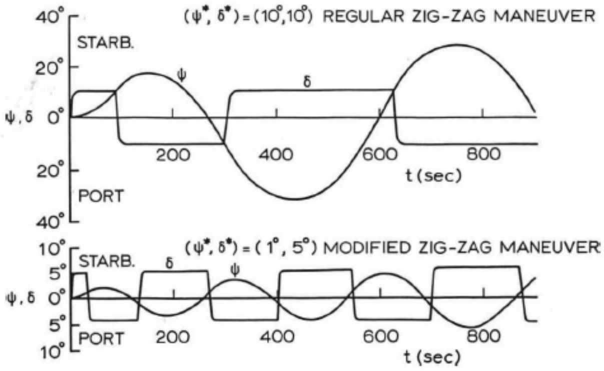

Fig. 7a An example of modified zig-zag maneuver.

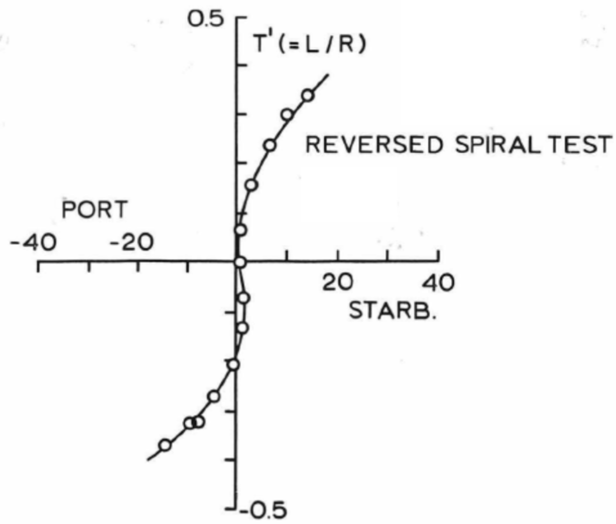

Fig. 7b Result of spiral test.

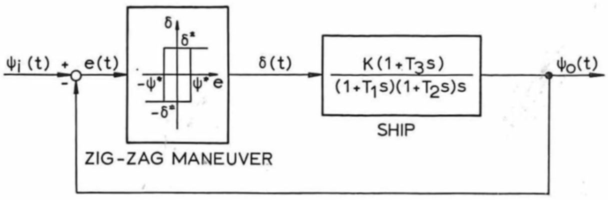

Fig. 8a

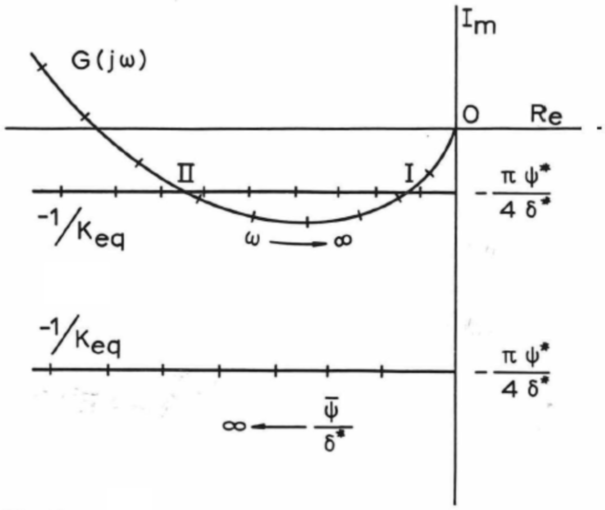

Fig. 8b

obtained by Fig. 8(b). Fig. 8(b) is a Niquist diagram of $G(j\omega)$ and $-1/\mathrm{Keq}$ where $|\mathrm{Keq}| = \pi\psi^*/4\delta$ is a describing function of the steering with hysteresis loop. Within the range where straight line $-1/\mathrm{Keq}$ intersects $G(j\omega)$, there exists a stable limit cycle, i.e., the modified zig-zag test becomes steady, and outside this range, the zig-zag test will diverge.

Sinusoidal maneuver

This method involves a sinusoidal change in rudder angle. Nomoto [7(a)] tried to obtain the frequency response of a ship by this test. One shortcoming of this method is that it is difficult to keep the ship's average heading constant. Moreover, it is not practicable to perform this maneuver at low frequency for which ship response is important. This is the main reason why we cannot depend solely upon the sinusoidal maneuver to obtain the frequency response.

Random steering test

In this test, the rudder angle is changed randomly and both the rudder angle and heading angle are recorded. From this record, the frequency response can be obtained. Koyama has tried this method on a cargo ship and obtained good results. In his case, the amplitude of the rudder angle was kept constant, and the time between switching helm angle was chosen at random.

Pull out maneuver

To obtain the height of hysteresis loop (viz. turning rate at zero helm angle) of a course unstable ship, Burcher [67] proposed the pull out maneuver. In this method, the ship is first kept turning at a specified rudder angle, then the rudder angle is set to zero and the successive heading angle is recorded until the ship's motion becomes steady. The steady turning rate thus obtained will of course be equal to the height of the hysteresis loop of the $r - \delta$ curve.

Parallel shift maneuver

In this maneuver, the ship is steered onto a new course parallel to the original. This method has been used by seamen to calibrate the ship's response for their own use. Nomoto and Karasuno [68] used this method to obtain the response function of a ship to the rudder angle. According to Nomoto, the best way to measure the response function is to use the sinusoidal maneuver for high frequencies, and the parallel shift maneuver for the lower frequency range. An example of a Bode diagram of the response function obtained is shown in Fig. 9.

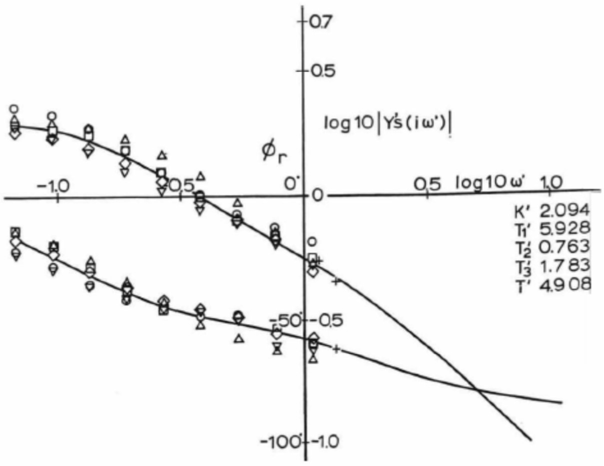

Fig. 9 An example of Bode diagram obtained by a parallel shift maneuver.

Course change test

In this method, the ship is steered onto a new steady course. The rudder angle, the time at which the rudder angle is changed, and ship's heading angle are recorded. An example is shown in Fig. 10. In this case, first, the rudder is put at 20°, then as soon as the ship's heading becomes 20° the rudder angle is reversed to –20° until the ship's turning rate becomes zero, the rudder angle is then put to zero. By this test, the ship's master can recognize the maneuvering characteristics of his ship.

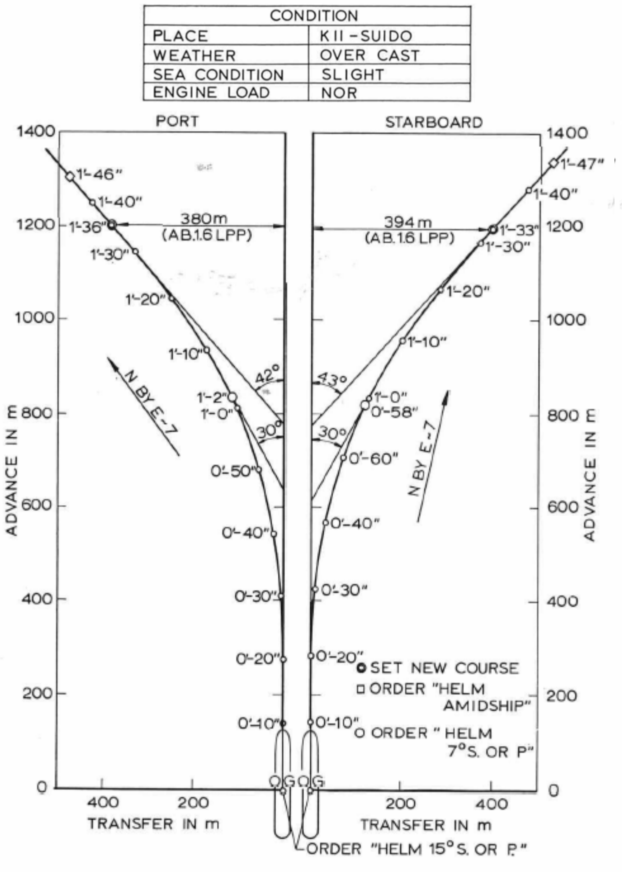

Fig. 10 New course test of a container ship.

Rudder effectiveness test at slow speed

This test is to examine the range of speed in which the ship can respond to the rudder when the engine is stopped and the ship is slowing down. A suggested method is to put the rudder angle at 35° and as soon as the ship begins to respond, the rudder is reversed to –35°; due to the effect of the reversed rudder angle, the ship will decrease its rate of turn and then reverse the direction of turn until it changes its heading angle 1° from the point where the ship reversed its direction of turn; then the rudder is reversed to +35°. This procedure is continued until it is judged that the ship no longer responds to the rudder. (see Fig. 11).

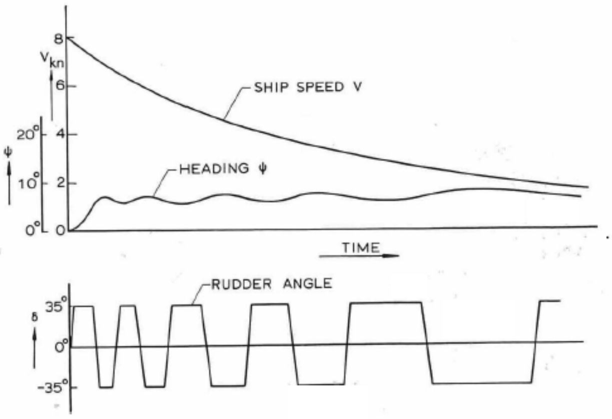

Fig. 11 Rudder effectiveness test at slow speed.

Motora and Fujino [66] classified steering motions into the following three groups:

a Course keeping maneuvers, (rudder angle less than 10 degrees).

b Course changing maneuvers, (rudder angle about 15°)

c Emergency maneuvers, (rudder angle 35°).

Using these categories, the above mentioned full scale test techniques will be roughly classified as follows;

a Course keeping	spiral test
	reversed spiral test
	modified zig-zag test
	pull out test
	low speed maneuver test
	parallel shift test
b Course changing	ordinary zig-zag test
	course change test
c Emergency	turning test
	ordinary zig-zag test at 35°.

Recently, IMCO has recommended that the masters of ships over 50,000 DWT should have a maneuvering booklet showing the ship's maneuvering characteristics, [69]. However, the standard methods of obtaining information that are to be included in the booklet have not been indicated. Therefore, it will be necessary to make up an international standard me hod for maneuvering tests. An interesting thing to be mentioned in relation to full scale measurement is the German experimental ship Meteor [70]. This ship was so designed that it can be used for full scale measurements for any purpose. For maneuverability, its steering gear is suspended by a dynamometer together with the rudder so that rudder force and torque can be measured during test runs. Results of the measurements are expected to be very valuable.

Model test techniques

Captive model test technique

Captive tests measure the hydrodynamic forces and moments acting on a model ship which is connected to and forced to move by a dynamometer. The following two techniques are common practice:

1 The rotating arm technique forces a model round a circular course with any desired drift angle. This technique has long been used and various establishments in

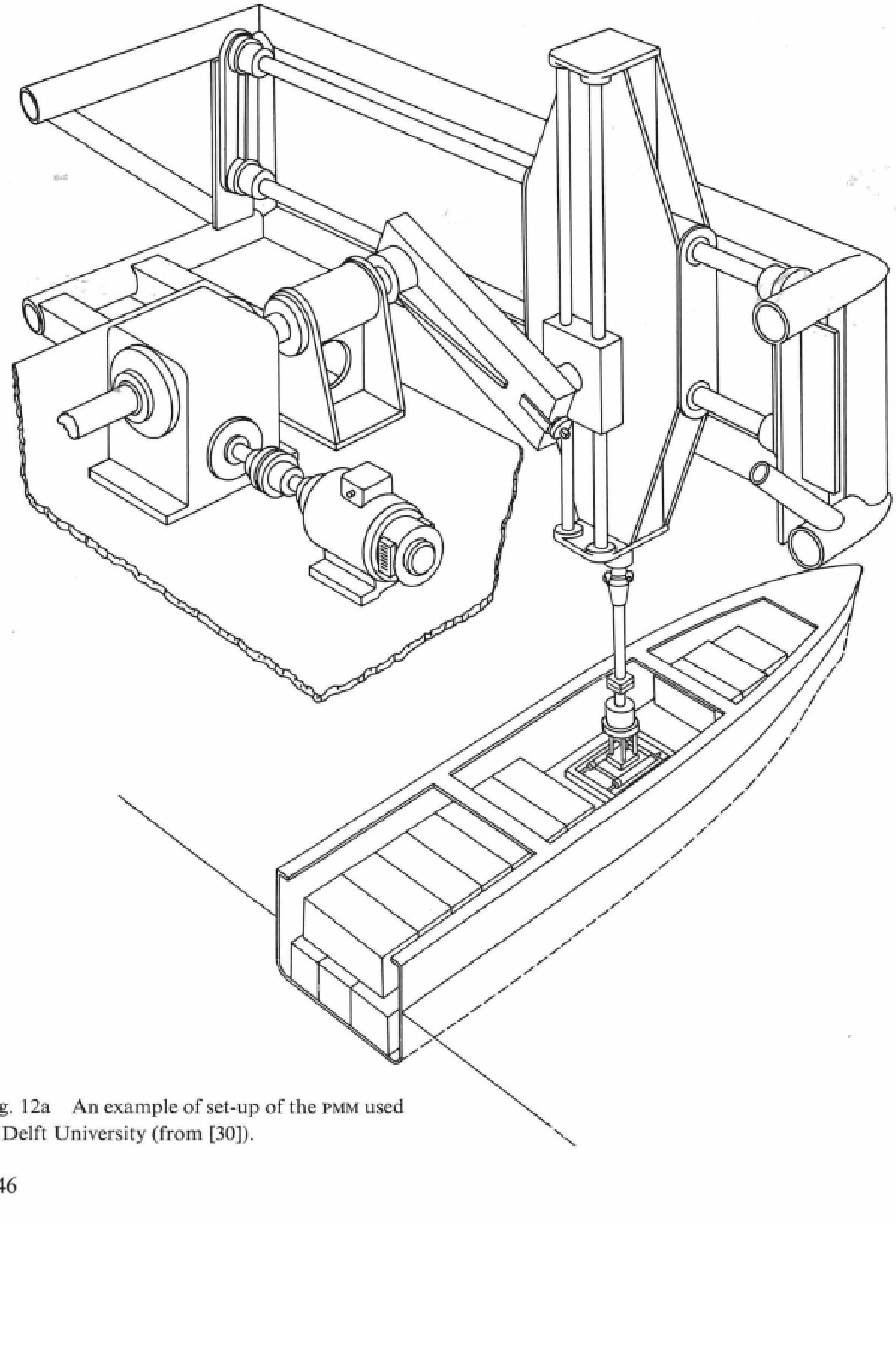

Fig. 12a An example of set-up of the PMM used at Delft University (from [30]).

the world own this facility. Among them, the ones at the Paris basin, AEW, Davidson Laboratory and NSRDC are famous. Recently, it was reported that the Krylov Institute has installed a high speed rotating arm [71]. As this technique is common, a detailed explanation will be omitted. For a detailed explanation, see [59].

2 The PMM (planar motion mechanism) technique forces a model to sway and yaw, and measures the hydrodynamic forces and moments. This technique was first used by Gertler [10, 11] for the measurement of stability derivatives of the depth control of submarines in the early 1950s at DTMB. Since then, this technique has been used to obtain derivatives for the steering motion of surface ships with a horizontal type PMM, and they are used at HyA, Delft University, University of California, University of Tokyo, AEW and Mitsubishi etc. Recently, HyA [72] completed a PMM for larger amplitudes. The University of Tokyo is also planning to use its *X–Y* carriage for large amplitude PMM [73].

An example of PMM apparatus used in TH Delft is shown in Fig. 12 (a). Typical forced motions of a model are shown in Fig. 12(b). The lateral force and the yawing moment are measured while the model is forced to oscillate, and derivatives are obtained resolving the force and moment into in-phase and out-of-phase components. Detailed explanations of PMM technique are given in [10, 11, 30, 38, 178].

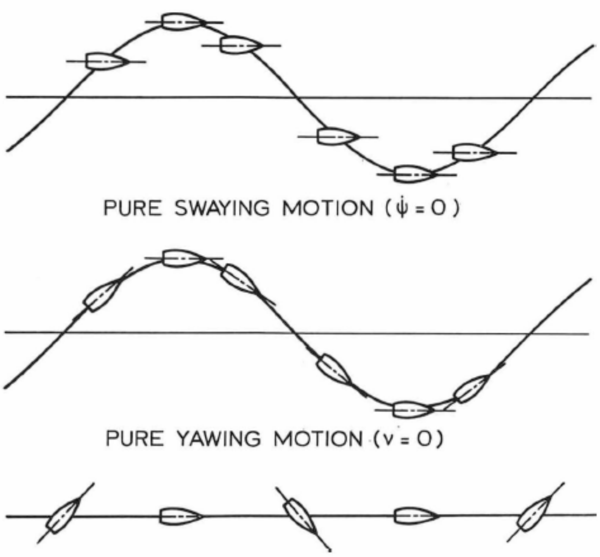

Fig. 12b Definition of motions.

Free running models

In the field of test techniques using free running models, there has been remarkable progress made in the telemetering of data and in the accurate measurement of the position of a model. Therefore model tests with free running models are widely conducted in establishments throughout the world.

Almost all of the full scale test techniques are applicable for free running model tests so that model test results can be used to predict the behaviour of full scale ships. Moreover, model tests can cover conditions that would be impractical with a full scale ship, and can cover a wide range of conditions that would involve too much time with full scale testing.

The ITTC maneuverability committee has conducted a cooperative test program on the Mariner type ship in which world-wide establishments conducted free running model tests using their own conventional experimental techniques. Results submitted were analyzed by Suarez [74]. An example of the results obtained is shown in Fig. 13. As seen in Fig. 13, there is some scatter between the data from different establishments, and in general, the turning radii for smaller models are larger than for larger models. This trend is more noticeable for the turning radii at small rudder angles. Fig. 14 is another example of data analyzed by Nomoto [75] in which the turning ability index K' is plotted against the model length. The same trend as mentioned above can be easily recognized.

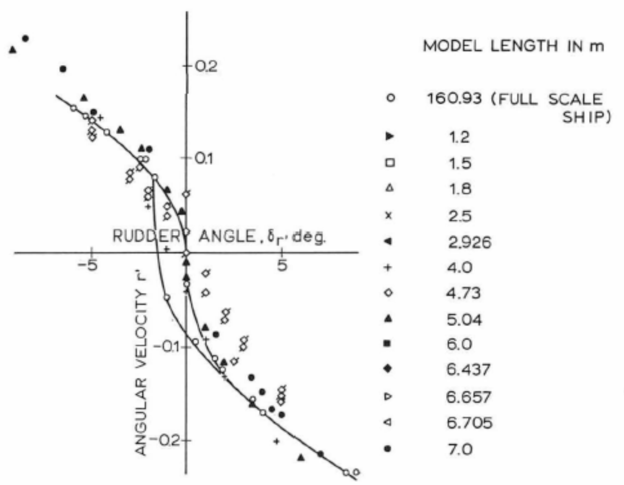

Fig. 13a Plot of spiral maneuver data δ_r versus r' for $U_A \approx 15$ knots.

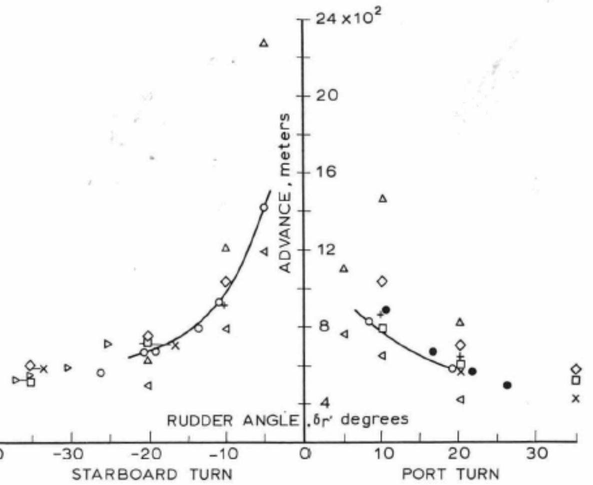

Fig. 13b Advance versus rudder angle for the speed range 13.3 knots $< U_A <$ 17.41 knots.

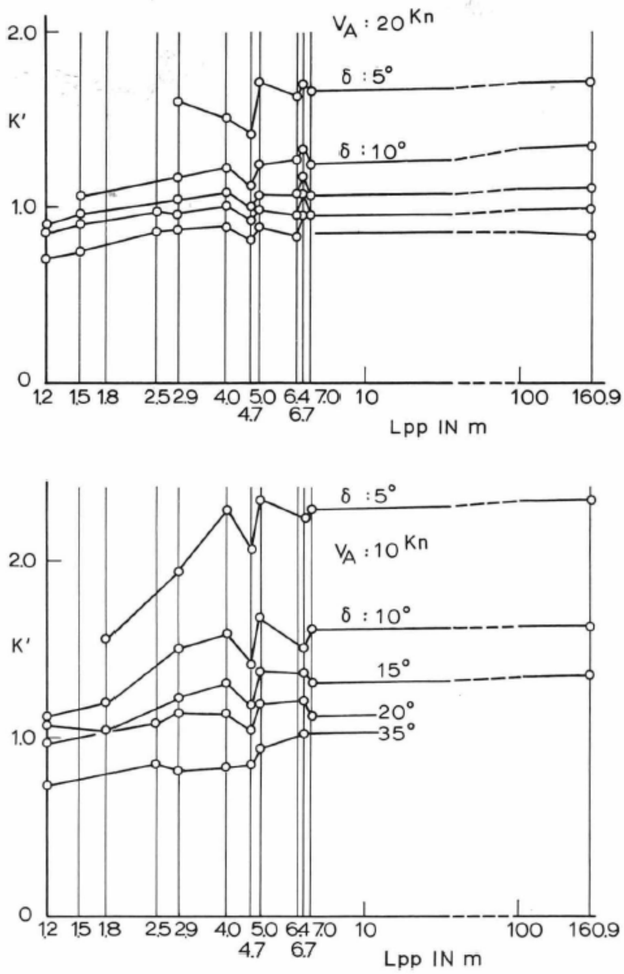

Fig. 14 Turning ability index K' derived from turning circle.

Ship-model correlation

As summarized by Vosper [76] and Thieme [82], in general, model ships tend to be more stable on course than full scale ships. viz., model ships are less turnable than full scale ships. This tendency is known to be not very pronounced at large rudder angles, but it is very notable at small rudder angles. The following points are thought to be the main causes of this trend.

Difference of propeller loading

The loading of a model propeller is larger than that of a full scale propeller due to the difference in the friction. This is known as the friction correction. Therefore, the slip stream of a model propeller is stronger than that of a full scale propeller. This increment of slip stream with model propellers will cause an increase in the fin-effect of the rudder, resulting in an effective increase of the deadwood or the skeg. This explanation was first put forward in [80]. It is also reported that the rotary derivatives increase at lower Reynolds numbers [77]. According to the data which Vosper [76] has referred to in his survey, in the case of twin screws with a twin rudder (Fig. 15), a stabilizing effect in model ships is very marked while in the case of two rudders with a single propeller (Fig. 16), the stabilizing effect is not so clear. Taking into consideration, that the rudder is not fully immersed in the slip stream, these data show that the increase of slip stream is one of the causes of the stabilizing effect in model ships.

Fujii [63] has conducted an experiment where an air-propeller was installed on a model to cancel the increased friction. Results obtained showed good agreement for the rudder torque in the transient state, but reasonable agreement was not obtained at steady turning rates. Such a discrepancy is supposed to be induced by a lateral thrust or a moment, produced by the air-propeller combined with the ship's motion. In restrained model tests, it is possible to give a suitable restraining force, so that the propeller loading becomes equal to that of a full scale ship [79]. However, such a change in the propeller loading does not give a full explanation of the difference of model and full scale data at steady turning rates. A proposal is also made to decrease the rudder area so that it generates, in the increased slip stream of the mode a rudder force equivalent to that of a full scale ship [80].

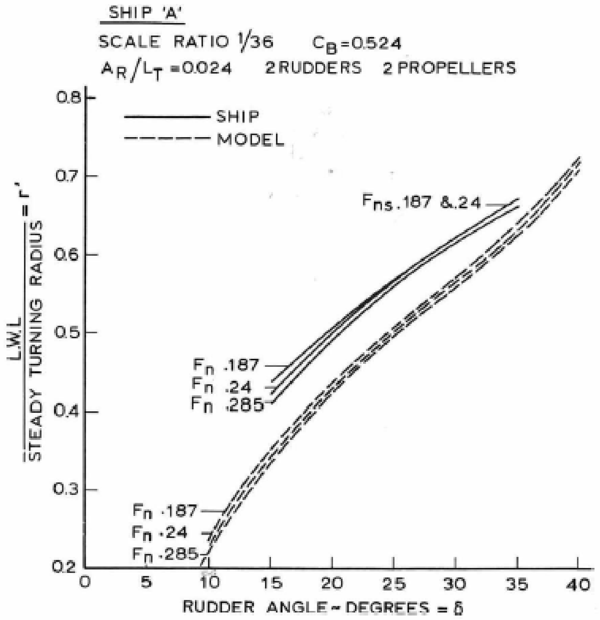

Fig. 15

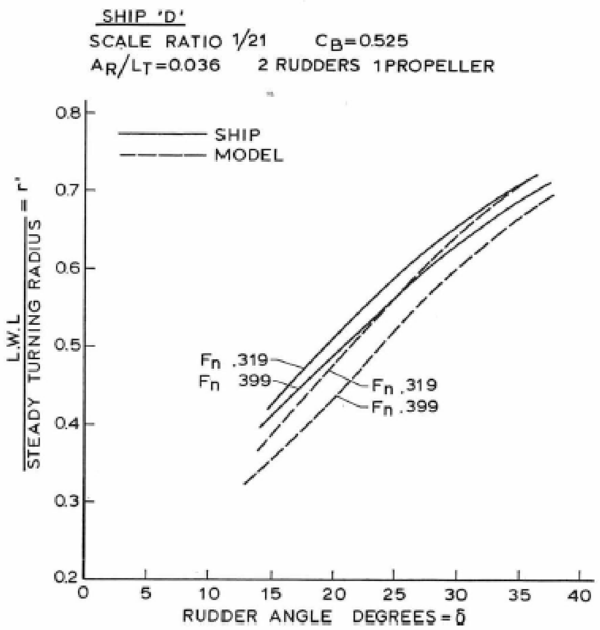

Fig. 16

Correlation of appendages

Since model appendages are immersed in flows with Reynolds numbers different from that of full scale ships and are fully affected by the thickness of the boundary layer, the correlation problem between model and full scale appendages is very complicated. Thieme [70, 81, 82] has given a broad survey on this problem as one of the tasks of the ITTC maneuverability committee. In the report, he has pointed out [81], that the difference in the Reynolds number at the rudder between a model and a full scale ship should be taken into account. Rakamarić [83] has reported a very interesting trial in which he tried to warm up the model rudder so that the results give an apparent increase in the Reynolds number.

Unusual phenomena associated with full and blunt bodied ship forms

As well as the above mentioned scale effect between a model and a full scale ship, there exist unusual phenomena in which model experiments give much smaller turning rates than full scale trials in the range of small rudder angles [84]. These phenomena are always associated with very full and blunt ships such as the recent supertankers. Such phenomena result in an apparent stabilization on course in the case of motion at low turning rates such as turning at rudder angles of less than 10 degrees or in zig-zag motions where the rudder angle is less than 10 degrees.

Particularly, in case of course unstable ships, it may happen that model data may indicate the ship is stable on course while the full scale ship is really unstable. In such a case, the prediction of full scale maneuverability by model experiments is practically impossible.

Some examples are shown in Figs. 17, 18 and 19. Fig. 17 is a result of reversed spiral tests on a supertanker in which the marks 'Δ' show the full scale data and the marks 'o' show the model data. In Fig. 17, the model data show that the ship is very stable on course in vicinity of $\delta = 0$ while the full scale data show that the ship is unstable on course, with an appreciable unstable loop.

In Fig. 18, the overshoot angle ψ_S and time lag T_L obtained from a zig-zag maneuver are shown for a tanker, 304 m in length. In Fig. 18, it will be noticed that at small rudder angles, the model data show remarkably small values for both the overshoot angle and time lag compared with the full scale data. Fig. 19 shows the results of K T analysis of the same ship. The same trend, that the model ship is apparently more stable than the full scale ship at small rudder angles will again be observed. These phenomena have been supposed to be induced by a flow separation at the stern of the model ships.

In recent years, however, these unusual phenomena have begun to appear even in full scale ships which are very blunt (L/B less than 6) and full (C_b greater than 0.83). In

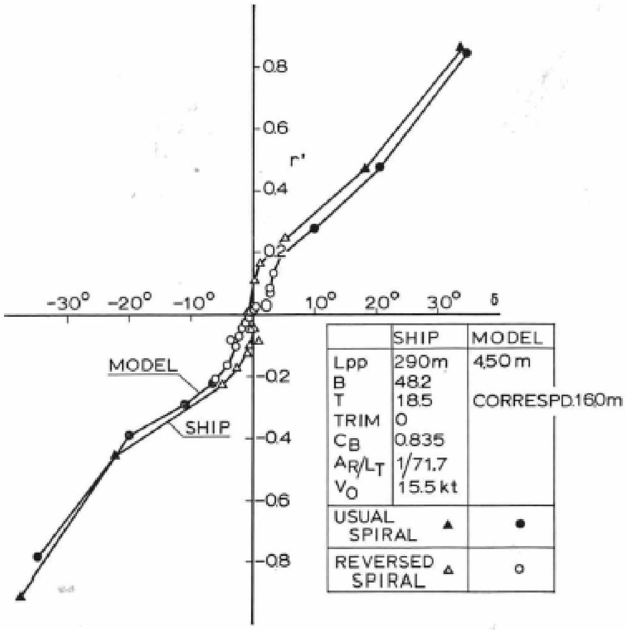

Fig. 17 $r' - \delta$ characteristics of a tanker and its model.

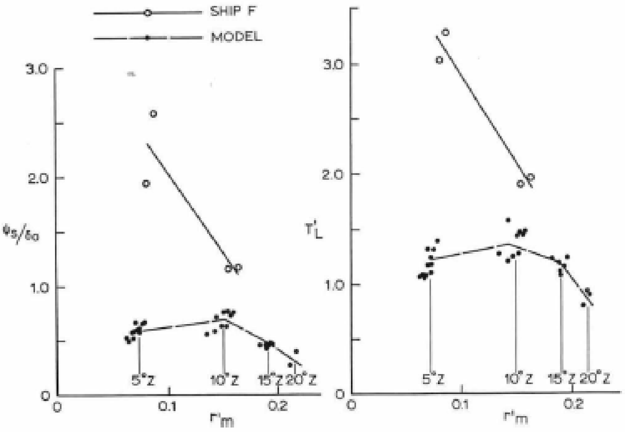

Fig. 18

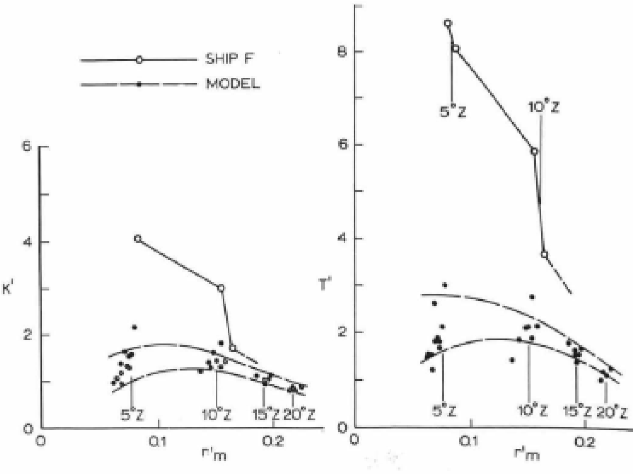

Fig. 19

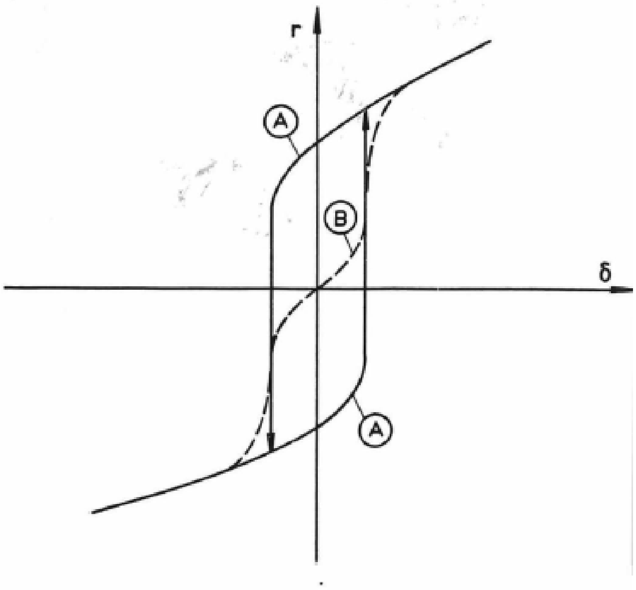

Fig 20

the case of full scale ships, these unusual phenomena often show a capricious and unsteady nature sometimes appearing and sometimes disappearing under the same test conditions. Some full scale ships were reported to have shown yawing without the presence of periodical external forces due to wind, waves or currents [86]. These ships are presumed to be as shown in Fig. 20. In Fig. 20, this ship is originally an unstable ship associated with an unstable loop (A in Fig. 20), but may take any value of turning rate within the loop A depending upon circumstances such as the present turning rate, hysteresis of motion etc. Since these test results are random, many plots will give an average line B which, as a result, shows that on the average this ship is stable on course.

A critical Reynolds number at which such unusual phenomena appear seems to depend on ship's fullness and bluntness. The more full and the more blunt, the lower the critical Reynolds number. Roughly speaking, it might be stated if C_b is less than 0.83, and L/B is larger than 6, the critical Reynolds number is just lower than that associated with full scale ships and the unusual phenomena appear only in model tests. However, if C_b is greater than 0.83 and L/B is less than 6, the critical Reynolds number becomes comparable to that of full scale ship tests as well. However, no reasonable proof has yet been given.

An attempt to reduce the unusual phenomena by attaching a pair of horizontal fins at the bossing of the propeller has been made [87].

Analysis of motion and definitions of maneuverability

History

As described in the introduction, a definition of the maneuverability is focused on the turning ability and only the turning radius, tactical diameter, the advance and the transfer have been used as the measure of the maneuverability. In 1944, Davidson [3, 4] introduced a new way of treating the maneuverability in which he used equations of motion about the body-axis. He also has given a clear explanation of the course keeping ability. He pointed out that if the solution of eq. 5 is written in the form of

$$r = Ae^{\lambda_1 t} + Be^{\lambda_2 t}$$

whichever of λ_1 or λ_2 has the smaller absolute value (say λ_1) gives the significant effect to r and it can be used as a measure of the course stability.
Since Kempf [5] introduced the zig-zag maneuver in 1944, the importance of the course stability and ship handling quality has attracted public attention. As is well known, Kempf himself proposed a standard to judge the handling quality of ships as follows: First a 10°–10° zig-zag maneuver is conducted on a ship, the rudder being switched four times, the distance run from the first execution of the rudder till the point when the ship's heading comes back to the original course after four switchings of the rudder is recorded. The distance thus obtained divided by the ship length is taken to be a measure. According to Kempf, this figure falls in a range of 6–10 for normal ships with reasonable handling qualities. Gertler and Gover [88] have proposed the use of the overshoot angle as a measure of handling quality.

Nomoto's K T analysis (frequency response analysis)

Nomoto [7, 8, 9] made a unique approach in analyzing Kempf's zig-zag test in which he made use of the theory of servo-mechanisms. He showed that the equations of motion of most ships were well approximated by first order equations and gave a clear explanation of the relation between the course keeping quality and the turning ability as summarized below:
First, the transfer function of r' to δ' is obtained by Laplace transformation from eq. 5.

$$Y'(p) = \frac{K'(1 + T_3' p)}{(1 + T_1' p)(1 + T_2' p)} \tag{12}$$

Expanding (12) for small values of p, we get

$$Y'(p) = K'[1 - (T'_1 + T'_2 - T'_3)p + (T'^2_1 + T'^2_2 + T'_1 T'_2 - T'_2 T'_3 - T'_3 T'_1)p^2 - \ldots] \tag{13}$$

On the other hand a first order approximation of eq. 5 is given as follows

$$T'\dot{r}' + r' = K'\delta' \tag{14}$$

The transfer function of (14) is

$$Y'(p) = \frac{K'}{1 + T'p} = K'(1 - T'p + T'^2 p - \ldots.) \tag{15}$$

Therefore, if we equate

$$T' = T_1' + T_2' - T_3' \tag{16}$$

eq. 5 is approximated by eq. (14).
Since this expansion is valid for small values of p, when $p \to 0$ the solution of eq. (14) coincides the solution of eq. (5), viz., eq. (14) gives the exact value when the time elapsed is sufficiently long. By the first order approximation, the maneuverability can be expressed by only two parameters K and T of which T indicates the time lag of the ship's response to the helm angle, while K indicates the turning ability. T is also very close to an inverse of the course stability index λ_1 with reversed sign. Therefore T is also a measure of the course stability of ships. K and T, named by Nomoto as the maneuverability indices, are now widely used in expressing the maneuverability of ships. Nomoto has also shown a method of obtaining the K and T indices from zig-zag test data, and this is now commonly used. In Figs. 21 and 22 examples

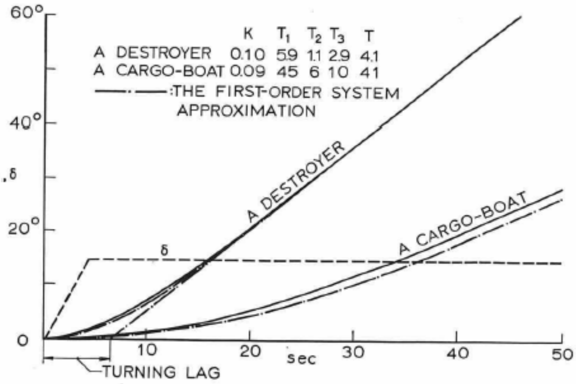

Fig. 21 First-order system approximation for turning transient.

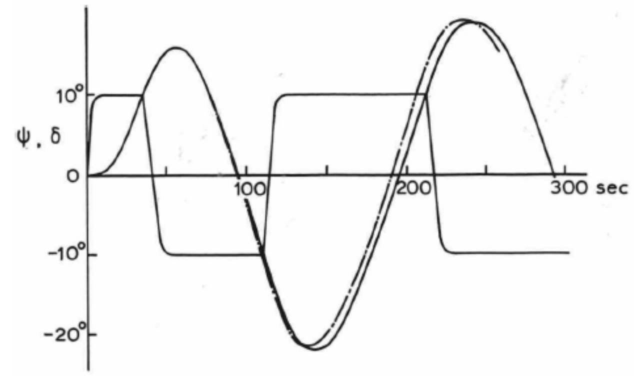

Fig. 22a Zig-zag test result for a full-loaded cargo boat.

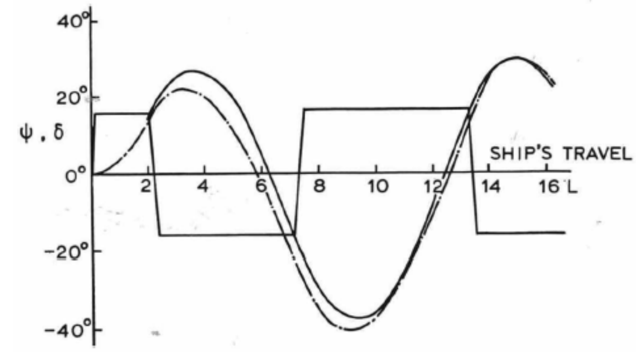

Fig. 22b Zig-zag test result for a supertanker.

of solutions of the first approximation are compared with solutions of the second order equation in the case of the turning test and zig-zag test.

Norrbin's P index

To define the rudder effectiveness, which is the ship's initial response to the rudder angle, Norrbin [90] proposed an index P which is the change of heading of a ship per unit rudder angle when the ship has run one ship length after execution of the rudder. The P index is obtained by putting the non-dimensionalized time t' in the solution of eq. 14 to be 1.

$$P = \left| \frac{\psi'}{\delta'} \right|_{t'=1} = K' \left(1 - T' + T' e^{-\frac{1}{T'}} \right) \tag{17}$$

Norrbin showed, based on many data, that P should be larger than 0.3 to secure reasonable rudder effectiveness. Nomoto [90] also proposed $P \geqslant 0.2$ for supertankers. The P index can be approximated as follows by expanding the $e^{-\frac{1}{T'}}$ term of eq. 17.

$$P \fallingdotseq \frac{1}{2} \frac{K'}{T'} \tag{18}$$

In Fig. 23, the P index (eq. 17), the approximate value of P (eq. 18) and full scale ship data are shown on a T' basis with K' as the ordinate.

Non-linear analysis

Linear equations fit fairly well over a wide range of turning rates in the case of course stable ships. However, in case of ships with poor course stability, linear equations do not give a good approximation due to the effect of non-linearity.
To overcome this problem, many attempts have been made to add a minimum number of non-linear terms to get a reasonable approximation as described in the chapter on equations of motion. Both r^3 type non-linear terms and Bech type $KH(r)$ non-linear terms seem to give reasonable results.

Phase plane analysis

Recently, phase plane analysis has become to be used in analyzing the response ability of ships to the rudder. In phase plane analysis, ship motion is transformed into an $r - \dot{r}$ plane, an example of which is shown in Fig. 24. Fig. 24 is a phase plane portrait of the zig-zag maneuver of a ship represented by a second order equation of motion. There are many ways of using phase plane portraits. Of these, an example given in [21] will be shown here, in which coefficients of non-linear equation of motion of the 2nd order are obtained.
First, put the slope of the phase plane portrait equal to s.

$$s = \frac{d\dot{r}}{dr} \tag{19}$$

then,

$$s = \frac{d\dot{r}}{dr} = \frac{\ddot{r}}{\dot{r}} \qquad \text{or } \ddot{r} = s\dot{r} \tag{20}$$

If the slope s is measured at constant δ, we get from eq. 9,

$$s\dot{r} = \tag{21}$$

Since $H(r)$ is known from a spiral test result, if the slope is measured at two points, we can get T_1 and T_2. Next,

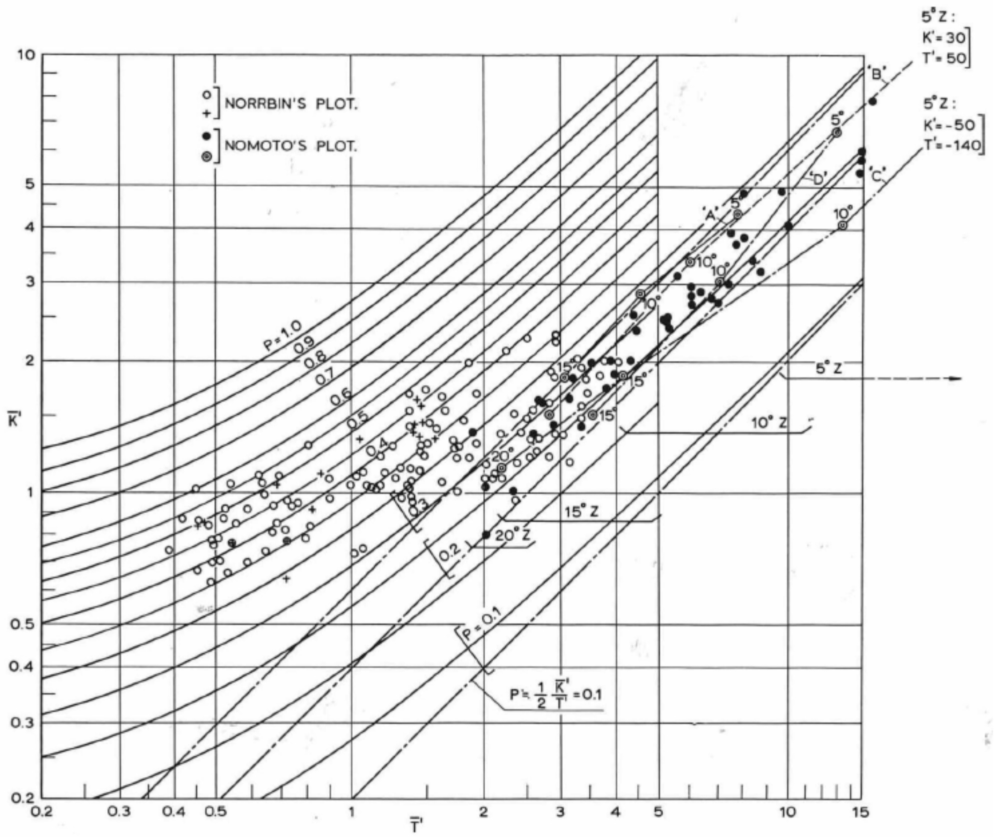

Fig. 23 Statistics of course change number *P* as obtained in zig-zag tests.

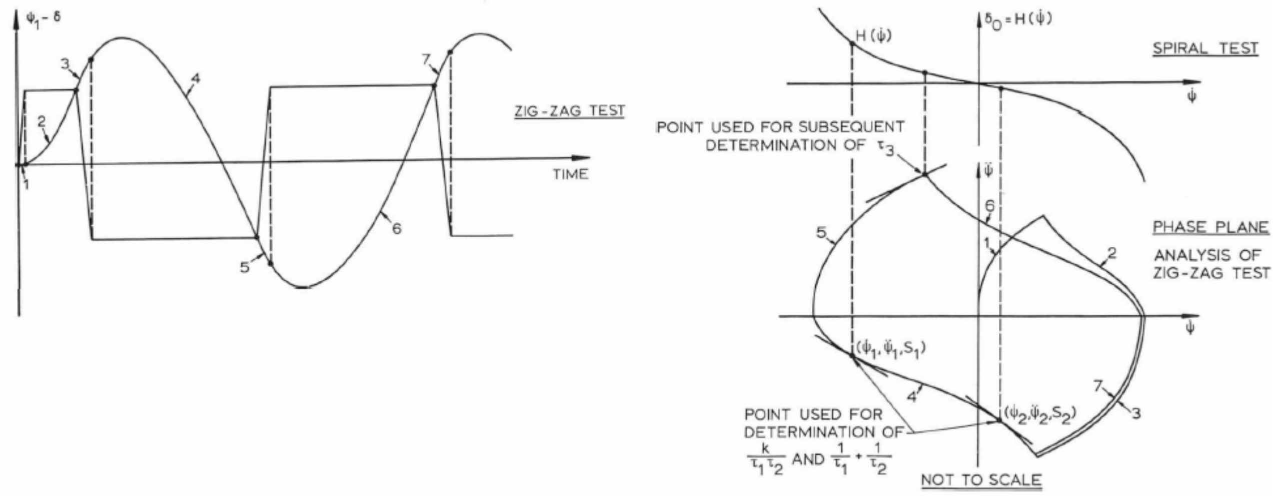

Fig. 24 Principles of phase plane analysis of zig-zag test.

if the slope is measured where the rudder is moving at a constant rate, since T_1, T_2 and $H(r)$ are known in eq. 9, we can get T_3. Norrbin has shown ways of analyzing ships which have strong non-linear tendencies [91, 92].

Simulation

The purpose of simulation of ship motions seems to be classified into two groups; one is for training crews or for studies of the human engineering in relation to control problems, and the other is for predicting ship motions.

For training and human engineering studies

This is simulated on a real time basis (usually using analogue computers) by which the ship's response to the rudder angle is computed and is displayed by the movement of a compass card or by a projection showing the changing view from the wheelhouse of a ship, so that the person steering feels as if he is really steering a full scale ship.

The equipment at TNO Delft [93] at NSMB [94, 179], and at SSPA [180], are famous. In the case of NSMB, the outside view is projected by a projector on top of the wheelhouse onto a cylindrical screen spreading around 360°. The silhouettes of islands and harbours are projected, their shapes being changed simultaneously by a servomechanism so that the ship's motion is more realistic. Maneuvering characteristics of an assumed ship can be easily changed by changing the setting of the computer. These simulators are not only useful in training crews for a specified size of ship or for specified maneuvering characteristics, but can be used for studies of the psychological effect of a ship's maneuverability on a crew, and of the response ability of the crew to the environments. The equation of motion used for this purpose is usually simpler than in the first case. Not exactly a simulator but for the same purposes, Esso at its training center at Grenoble France (Esso REM) [181], is using large sized ship models which are installed with realistic steering gear, engine telegraph and meters etc. for training the crew of supertankers. This method is handicapped by the fact that the time is also scaled down. However, it is said that this method is still usable for training crews in approaching buoys or in passing through narrow channels where they can try more adventurous steering than they would ever dare to try on a full scale ship, and they can experience the effect of bank suction and so on.

Prediction of ship motions

This method is to compute ship motions under steerage by making use of higher order non-linear equations, fitting higher order derivatives obtained from model experiments. Digital computers are usually used for this purpose. The purpose of this method is to predict ship motions before a ship is constructed or to predict motions of a ship under conditions which are too severe for a full scale ship to try. It will also be possible to extrapolate a limited amount of full scale data into a wider range of conditions. This method is also useful for autopilot designs. For the equations of motion, 3rd degree higher order equations as described in the chapter on equations of motion are commonly used [22, 95, 96 and 98]. The simulation of full scale maneuvering data by simple equations has also been tried [20]. Some examples of simulations are shown in Figs. 25 through 29. Fig. 25 is a result of simulation of the zig-zag test by Strøm-Tejsen [22], Fig. 26 is a comparison of simulation by a linear equation and a non-linear equation by Inoue [97], Fig. 27 is a simulation of the effect of wind on a turning test by Ogawa [95], Fig. 28 is a simulation of the initial stages of steered motion of a ship by Eda & Crain [98], Fig. 29 is a simulation of the spiral test by Norrbin [96].

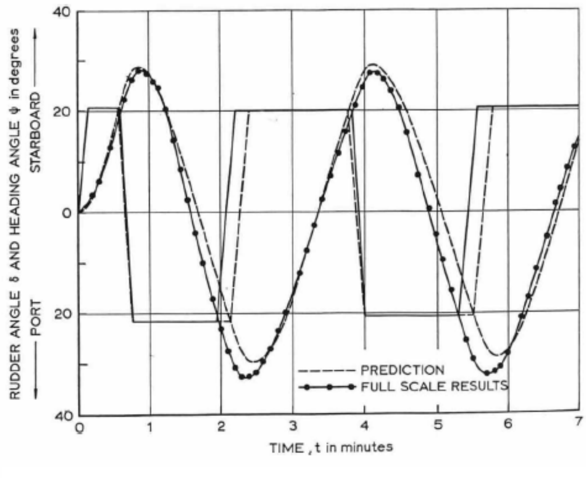

Fig. 25 Comparison of zig-zag maneuver from full-scale trials and prediction from model tests; 15-knot approach speed (from [22]).

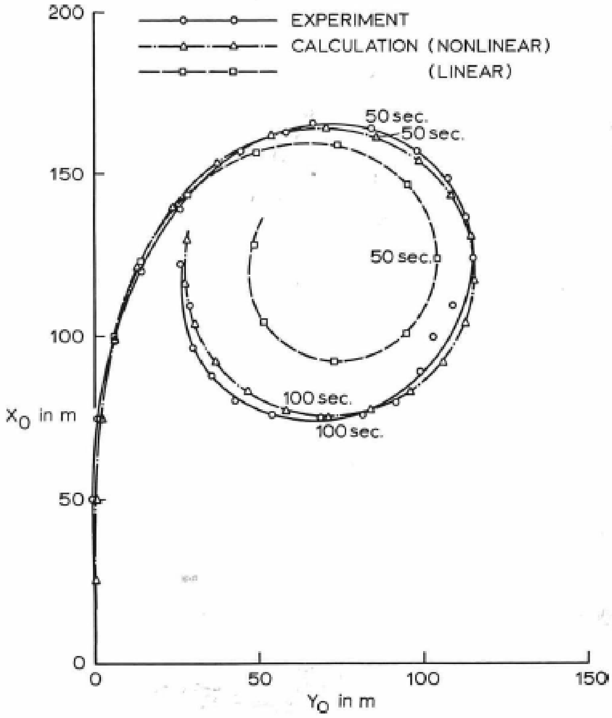

Fig. 26

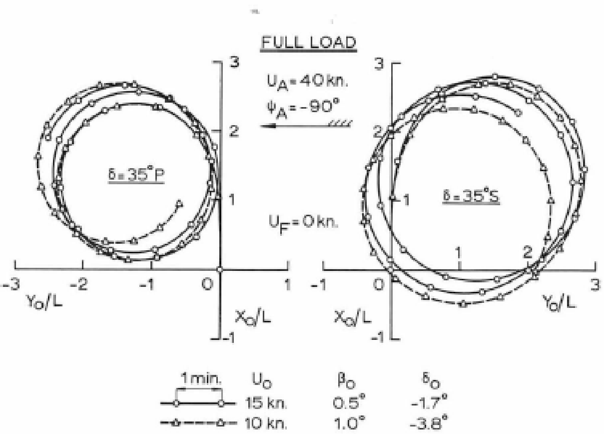

Fig. 27 Simulation of turning in wind.

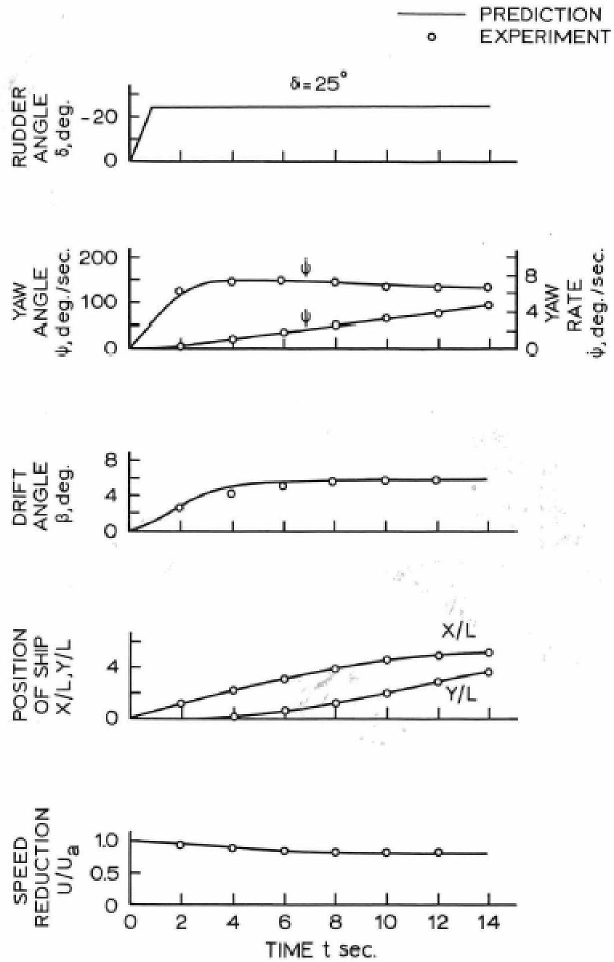

Fig. 28

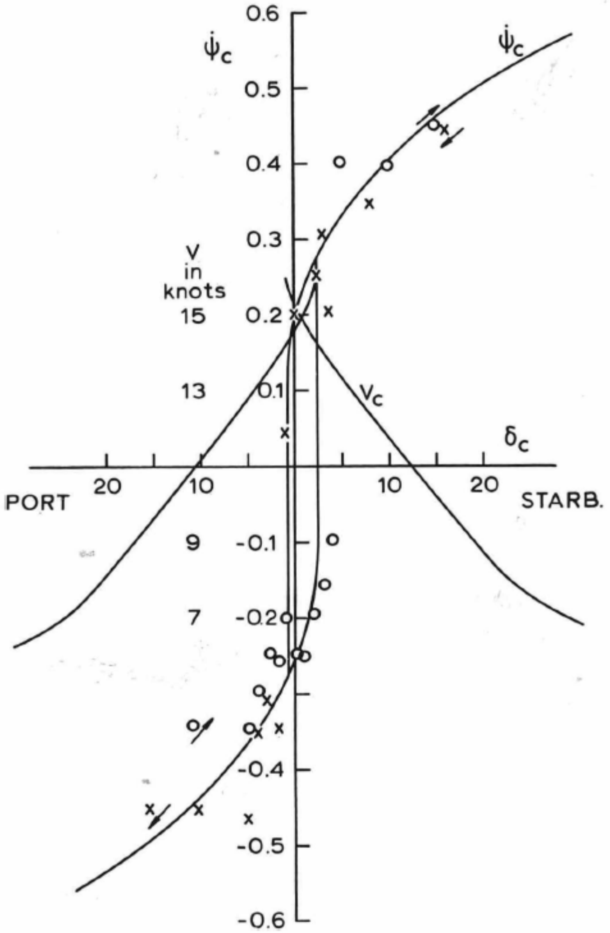

Fig. 29 *T/T* Malmöhus- $\dot{\psi}_c$ (δ_c)-diagram from spiral tests in deep water. Comparison of full scale trials (x, 0) and computer prediction (————).

Simulation of the harbour traffic

Sugisaki and Watanabe [100] tried to use a digital computer to simulate traffic condition in a strait and obtained the traffic capacity of the strait. In these trials, it is assumed that a ship has its own closed domain which consists of an ellipse 8 ship lengths long in the front, 4 ship lengths wide, and an ellipse 2 ship lengths long in the rear. As soon as another ship enters this domain, the ship should change its heading by 15° (or 30° if necessary) in a direction such that the other ship is excluded from the domain. In the case where any change of heading is impossible, the ship should slow down until the other ship is excluded from the domain. The loci of ships are successively computed, assuming ships arrive at a starting line at the end of the strait in random time intervals with a specified distribution in the transverse direction.

According to the result, the average ship speed goes down as the average density of ships per area of the strait increases. This relation is shown in Fig. 30.

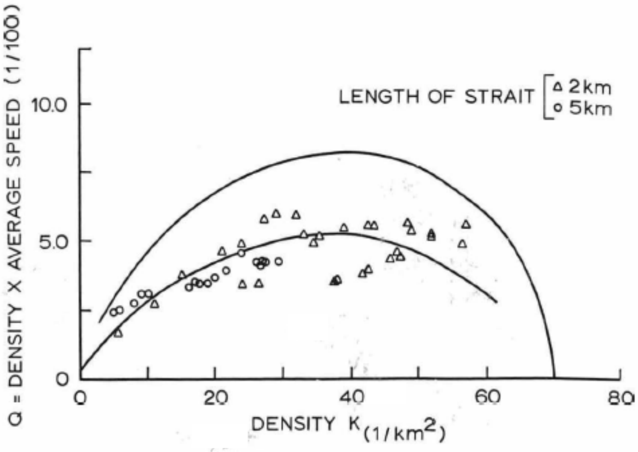

Fig. 30 Simulation of the traffic capacity.

Automatic control and routing

The purpose of the automatic control of ships was basically to maintain ships on a straight course. However, in recent years, its range of usage has widened to cover the routing of ships in a wide sense and the improvement of safety and reliability as summarized in the following:

a Improvement of the efficiency of a system under consideration,

b Improvement of safety and reliability,

c Decreasing man labor.

Automatic control in the ocean

a Selection (Determination) of the route

It is a difficult problem to select an optimum route from port to port under varying environmental conditions since the evaluation depends on the kind of ship and the kind of cargo. In recent years advice on the optimum routes for ships based on weather forecasts has become a commercial service. It is expected that every ship will select its optimum route by the aid of a computer on board the ship. In the case of a routing system in use in the United States of America [101] evaluation of the optimum is based on minimizing the time to get to the port of destination, and the wave forecast for five days is used as input data. In this method, the Atlantic ocean is divided into grids and significant wave heights and directions are given for each mesh. The characteristics of the ship are represented by a simplified model in which the loss of ship speed is given as a function of significant wave height and relative direction of the waves. A ship's course obtained by a routing equation under the condition of minimum navigating time is delivered to the ship. At present, the captain gives the final decision based on this information.

b Automatic control onto a predetermined course
When the optimum route is decided, the next problem is how to keep the ship on course under effects of wind, waves and currents. This technique can be called automatic control in a narrow sense. This has been done in such a way that the position of the ship is occasionally measured, and the ship is controlled on a straight course until the next measurement. In recent years, as radio locating devices or navigation satellites have become available, it is becoming possible to feedback the ship's position frequently or continuously. If there are no disturbances due to the environment, the best control has a minimum deviation from the predetermined course. Existing auto-pilots give excellent performances for this purpose [188]. However, under the influence of perpetual wind and waves, minimum deviation does not necessarily give the optimum efficiency for a system. Koyama [102] defined the optimum efficiency of automatic control as 'minimizing the energy loss in advancing under the influences of wind and waves'. He offered an evaluation function as shown below and defined that an auto-pilot which makes this evaluation function a minimum has optimum performance.

$$J = \hat{\theta}^2 + \lambda\hat{\delta}^2 \qquad (22)$$

where
$\hat{\theta}^2$ is the square mean of the deviation of heading
$\hat{\delta}^2$ is the square mean of the rudder angle
λ is a weighting function.

Eq. (22) shows that, if the control is too intense, although θ will decrease, δ will increase, resulting in an increased energy loss due to the drag of the rudder, and that if the control is too weak, although δ will decrease, θ will increase resulting in an increase in the course length [103, 104, 105, 106].
According to Koyama, λ is about 8 for Mariner type ships. This means that the intensity of optimum control is rather small compared to what had previously been thought reasonable. In making J a minimum, the most difficult problem is how to filter out higher frequency disturbances which are the cause of frequent rudder movements. As is well known, the simple method of allowing a certain amount of play in the detection of the heading angle causes a delay resulting in the decreased damping of the system. Many methods such as putting in a dead band or putting a restriction on the rudder amplitude have been tried and these are the speciality of each existing auto-pilot.

Automatic control in a closed waterway

a Automatic guidance
The necessity of automatic guidance on a predetermined network of courses in a harbour area to avoid collisions and strandings seems imminent. There appear to be two methods: one is to control the ship by a land based system, the ship only receiving and following the signal, and the other is to give a specified course to a ship and allowing it to follow that course using its own system. In either case, since the allowable error in position is very small compared to the case of ocean routing, it will be necessary to make frequent positional checks and to make corrections taking into account the ship's motion characteristics and the effects of wind and current. There have been many studies in this field [111, 112, 113, 182, 183].

b Assistance to the manual steering
Usually a ship is controlled manually in a harbour area where traffic is busy. However, in the case of modern supertankers, ship motion is so sluggish, due to the tremendously large time constant, that it is beyond the range of human sensitivity to detect such comparatively slow changes of circumstance. To overcome this fact, it will be possible to assist human sensitivity by displaying an amplified turning rate (for instance) so that the helmsman can detect the ship's motions much easier. A method of displaying an amplified approaching speed for a ship to a pier is now in practical use. In this connection, Motora and Koyama [107, 187] have suggested a method in which an automatic control to stabilize a ship is applied to an originally unstable ship. The ship therefore responds to the helm angle which is modified by the automatic control from the original helm angle which the helmsman has taken.
In this way, the helmsman feels as if he is steering a stable ship which feels very easy to steer. Moreover, since the ship is originally unstable, it can turn quite well when the automatic control is shut off if necessary. In the above mentioned cases, a closed loop system which contains both the ship and helmsman should be considered [108, 109].

A motion predictor which can display the result of a contemplated steering maneuver at any instant will be a great help for a helmsman or captain in an emergency to judge whether the action he is going to take is adequate [184, 185].
Norrbin [186] made a broad survey of this problem.

Maneuverability in restricted waters

Research works into the maneuverability in restricted waters have been done in relation to navigation through the Suez and Panama canals and inland waterways. Among them, the work by Baker [114] dealing with general problems of restricted waters, a series of experiments at the Paris Model Basin [123, 124], general descriptions by Smitt Stiebitz [115 to 119] and extensive experimental studies at DTMB [120, 121, 122] are famous. In accordance with the appearance of supertankers, the problem of restricted waters becomes very important because most coastal water areas can no longer be considered as deep water. In view of the increasing importance of the maneuverability in restricted waters, the ITTC maneuverability committee has recommended taking this problem as one of its tasks, and Motora and Fujino [126] made a review at the 11th ITTC on this problem. At the 12th ITTC, Norrbin [127] gave a review on new problems in this field, and Motora [128] tried to review Japanese work in this field.

Maneuverability in shallow water

a Hydrodynamic force and moment in shallow water
The waterflow around a ship in shallow water differs from that in deep water, a relatively low pressure being generated at the bottom, resulting in an increased draft. This phenomenon is well known as 'squat'. Other than squat, changes in the added mass, yaw damping and sway damping etc. appear due to the change of flow around a ship as the bottom clearance decreases. There are two theories for studying the hydrodynamic forces in shallow water: low aspect ratio wing theory and slender body theory. Kan and Hanaoka [131] have obtained the lateral force acting on a flat plate of specified draft by making use of the low aspect ratio wing theory. They treated infinite images of a flat plate in which the breadth is twice the draft and the spacing is twice the water depth. The result was expressed by a coefficient k_F which is the ratio of the lateral force at depth H, Y_H, to the lateral force at infinite depth Y_∞

$$k_F = \frac{\psi H}{\pi^2 d}\int_{-1}^{1} \cos h^{-1} \frac{\cos \dfrac{\pi\zeta}{2H/d}}{\cos \dfrac{\pi}{2\pi/d}}\, d\zeta \qquad (23)$$

It was also shown that the ratio of added mass and added moment of inertia are also equal to k_F. Newman [132] and Tuck [133] have investigated the slender body theory. Newman has pointed out that the flow at the bow and stern is not two-dimensional, and has separated the flow into an inner and outer region, and has matched the two kinds of flows. The result was given by a coefficient which is exactly the same as in eq. (23).

$$k'_F = \frac{F_i(k, H)}{F_i(k, \infty)} = \left[k\frac{d}{H}\beta_i^{-1} - \frac{}{8 \log \cos \dfrac{\pi}{2}\dfrac{d}{H}}\right]^{-1} \qquad (24)$$

$$F_i = \{m_y, J_z, Y, N\} \quad \beta_i = \left\{1, \frac{3}{8}, 4, 2\right\} \quad k = 2d/L$$

Comparing this result to Kan and Hanaoka's result, both agree quite well when $k = 0$. At values other than $k = 0$, for instance $k = 0.1$, there are slight differences in m_y, J_z and N (see Fig. 31).

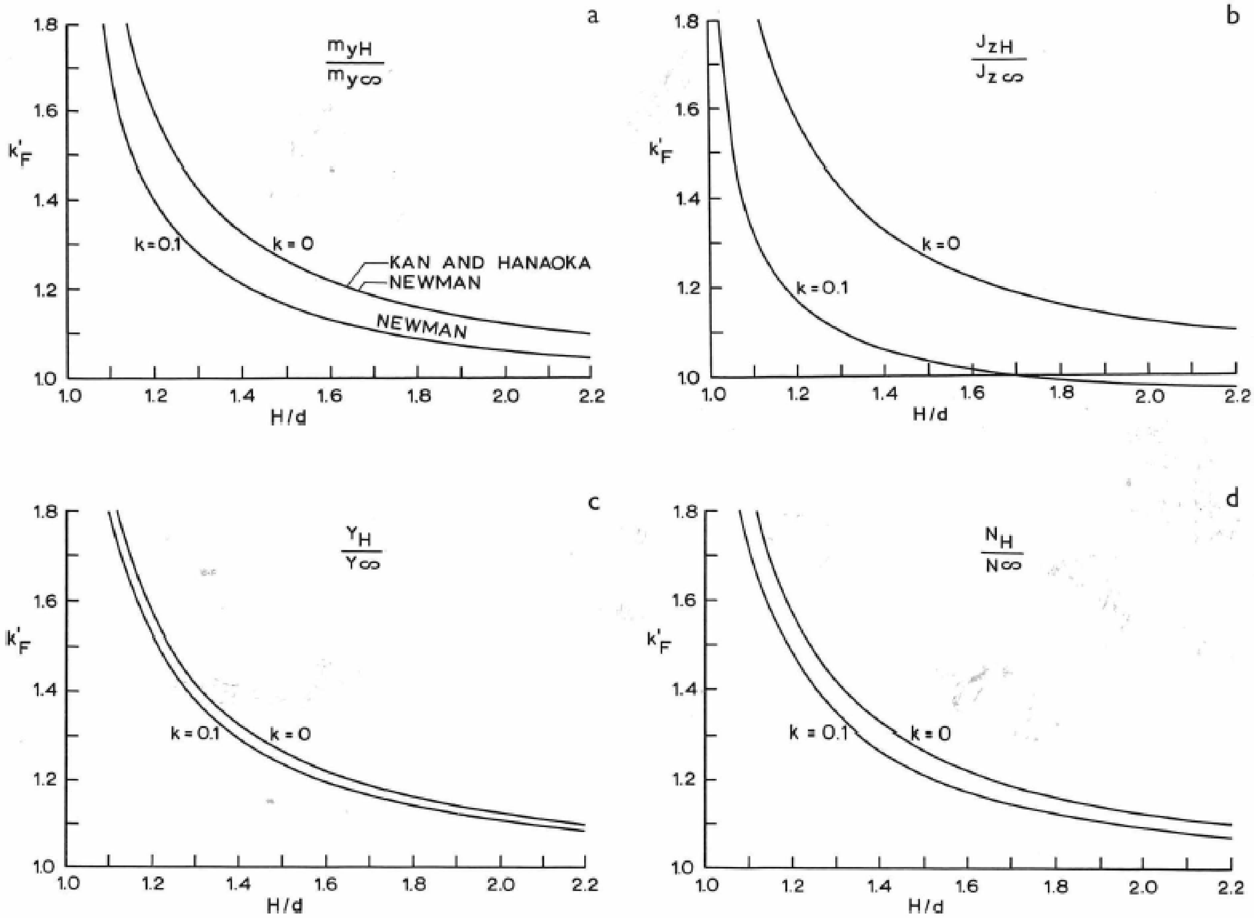

Fig. 31a, b, c, d Shallow water effectiveness coefficients (from [176]).

Inoue and Murayama [135] also made a calculation of the hydrodynamic force by low aspect ratio wing theory. The result lies in between the values for a flat plate and a circular cylinder obtained by Kan and Hanaoka (see Fig. 32). Experimental values have been obtained by Brard [123] and Fujino [129]. Fujino measured added mass, added moment of inertia and rotary derivatives in a shallow basin by making use of the PMM technique. Results are plotted in Fig. 32 and are compared with the theoretical value of Inoue.

b Effect of shallow water on the maneuverability

It has been found by experiments that due to the change of the flow around a ship in shallow water, a ship tends to be more stable on course and less turnable in shallower water. This tendency is also explained theoretically [131]. For experimental data, full scale data by Motora and Couch [137] and model experimental data by Baker [114], Brard [123], Bindel [124], Koseki and others [139] and by a Japanese research organization [145] are available. There are also simulation results based on model experiment data by Fujino [129, 130], Norrbin [96] and Eda and Crane [143].

Summarizing these results, it can be concluded that a ship tends to be more stable on course and less turnable as the water depth becomes shallow except at a middle depth where it is reported [139, 129] that a ship becomes less stable and more turnable than in deep water. An example is shown in Fig. 33. Fujino obtained a similar

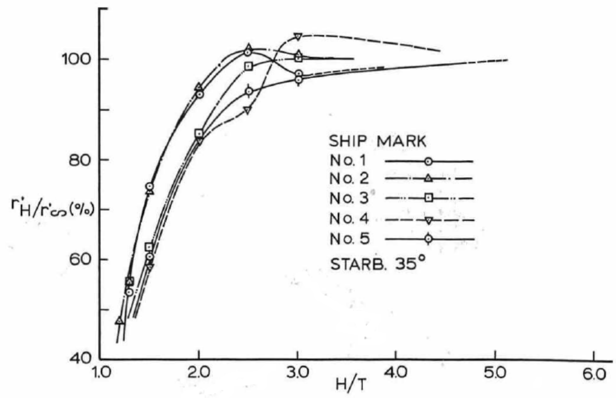

Fig. 33 Effect of water depth on the turning rate.

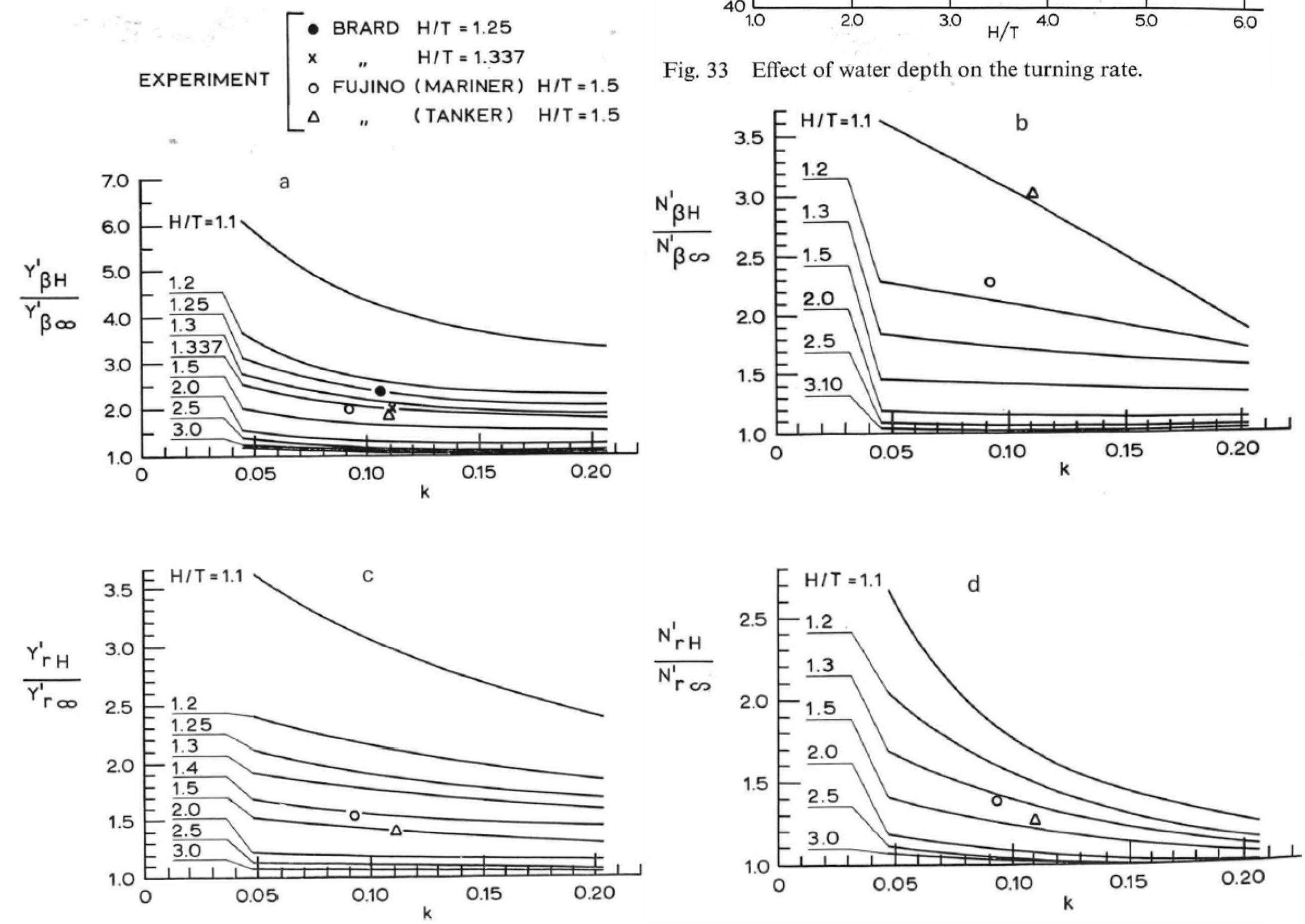

Fig. 32a, b, c, d Comparison of theoretical and experimental values of shallow water effectiveness coefficients (from [176]).

result by a simulation based on the derivatives measured by PMM technique.

Maneuverability in narrow channels

a Hydrodynamic force and moment.
When the waterway is narrow as well as shallow, the blocked waterflow around a ship becomes faster than in the case of shallow water only. If a ship is off center in a channel, viz. in case of off-set navigation, due to asymmetry, the ship will be acted on by a lateral force and moment pulling the ship towards the near bank and pushing the bow of the ship away from the near bank. This force and moment have been called bank suction. Inoue and Kijima [136] obtained bank suction forces by Bolley's low aspect wing theory (see Fig. 34). In Fig. 34, the ratio of hydrodynamic force and moment in a channel of width W and that in unrestricted width but the same depth is shown. There is also much experimental work, among which an extensive experiment conducted at DTMB [120, 121, 122, 141] in relation to a modernization of the Panama Canal, is famous. Fujino [130] measured stability derivatives and the bank suction of ships in canals making use of the PMM technique. Table 4 is an example of his measurement on a Mariner ship model. Y_η' and N_η' are the normalized bank suction force and moment. In measuring Y_β' and N_β' in a channel by the PMM technique, it is necessary to correct for the effect of bank suction. From Table 4 it will be noticed that values of the derivatives in general increase as the width of the channel decreases.

b Effect of restricted width on the maneuverability
While a ship tends to be more stable on course due to increased derivatives, bank suction acts to make a ship unstable. Therefore, as a consequence, a ship will become less stable on course in a narrow canal. This trend is emphasized due to squat when the ship speed increases. Moody [121, 122] has conducted an extensive experimental study in this field. Brard [123], Bindel [124] and Hooft [147] conducted extensive experiments by free running models through model canals and obtained a critical speed range above which a ship cannot navigate safely through a canal.
Simulation of ship motions in canals based on empirical derivatives has been done by Fujino [130] and Eda and Crane [143]. According to Fujino, both the Mariner ship and tanker which he tested became unstable in a canal

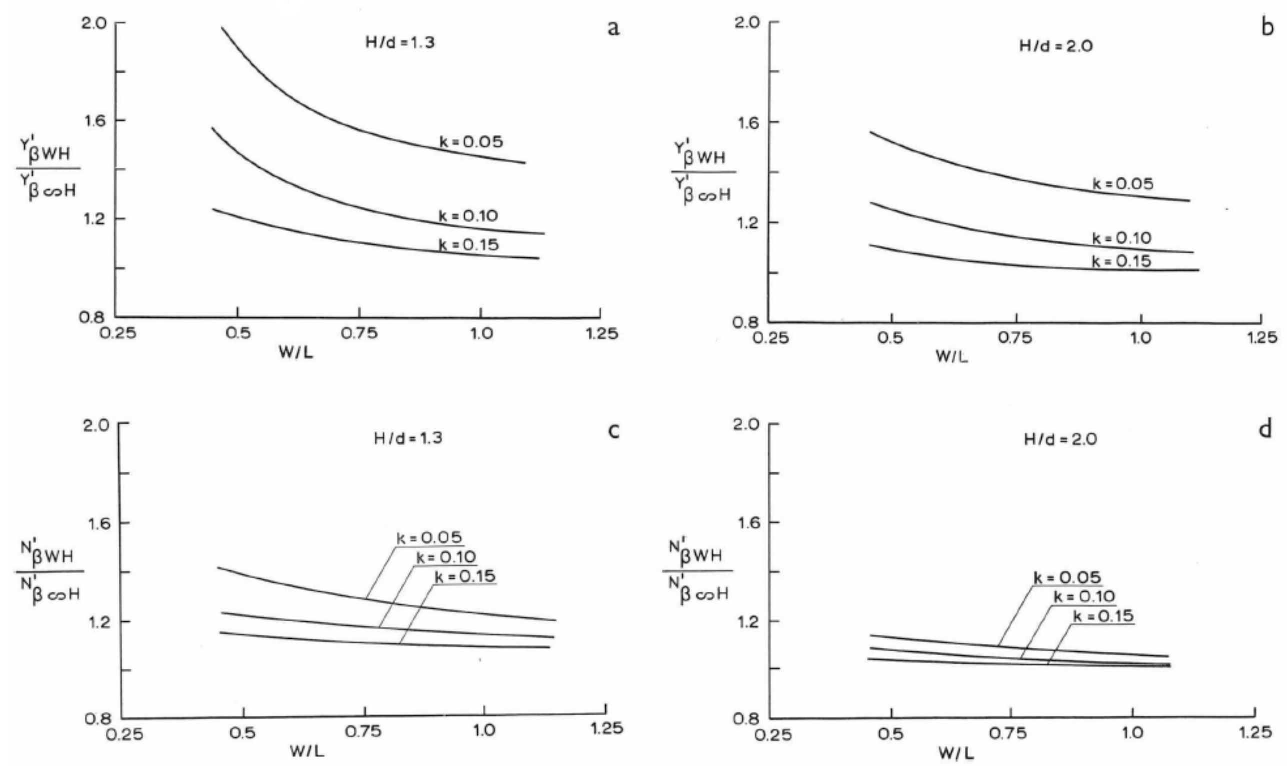

Fig. 34a, b, c, d Restricted width coefficient (from [176]).

Table 4 Hydrodynamic coefficients of a Mariner Class ship in a narrow channel (Fn = 0.0905) (From [130])

Type of test		$H/T = 1.3$			$H/T = 1.5$			$H/T = 1.9$		
	W/B	5.56	4.17	2.78	5.56	4.17	2.78	5.56	4.17	2.78
Forced yaw test	$m'+m'_y$	26.3	30.9	35.7	23.8	25.0	25.8	19.8	20.2	21.2
	Y_β'	57.0	73.7	96.7	30.1	35.6	41.6	20.3	21.8	23.2
	$N_{\dot\beta}'$	–0.469	–0.555	–0.699	0.134	–0.012	0.015	0.041	–0.023	0.124
	N_β'	12.5	14.2	18.4	8.50	9.86	12.08	5.88	6.67	7.23
	Y_r'	2.17	4.37	7.78	–1.42	–0.362	2.21	–3.60	–3.54	–2.57
	$Y'_{\dot r}$	–2.17	–2.62	–3.41	–1.34	–1.17	–1.47	–0.676	–0.722	–0.826
	N_r'	–4.93	–5.47	–7.27	–3.62	–3.75	–4.43	–2.74	–2.90	–3.07
	$I_z'+J_z'$	1.25	1.41	1.82	1.24	1.28	1.42	1.11	1.16	1.21
Oblique tow test	Y_β'	82.6	98.2	136.1	39.5	42.6	50.5	22.7	24.5	24.6
	N_β'	9.34	10.6	15.2	8.17	9.31	11.91	6.39	7.24	7.92
Rudder force measurement test	Y_δ'	4.45	4.63	4.78	3.68	3.92	4.37	3.60	3.67	3.59
	N_δ'	–1.94	–1.93	–2.36	–1.78	–1.89	–2.06	–1.52	–1.66	–1.76
Asymmetric hydrodynamic force measurement test	Y_η'	6.99	13.4	33.5	4.23	9.20	27.4	2.35	5.35	13.31
	N_η'	–1.14	–3.24	–12.45	–0.689	–1.770	–5.012	–0.305	–0.846	–2.43

Note: All figures must be multiplied by 10^{-3}.

due to the effect of bank suction. He also showed that these ships may easily be stabilized by applying a simple automatic control proportional to the heading angle. This means that these ships are manually controllable in a canal even though it causes them to be unstable on course. It is also interesting to know that a rate control is useless in stabilizing a ship in this case.

Squat

Due to increased flow velocity around a ship in shallow water and in canals, a ship tends to squat. The amount of squat is greater when the water depth is shallower and the width of the channel is narrower. Particularly in narrow and shallow canals, ships sometimes touch the bottom. Therefore, it is necessary to keep a ship's speed lower than the critical speed. Theoretically, the squatting force has been studied by Constantine [125] and Tuck [133, 134]. Tuck has calculated the squatting force of a slender ship in shallow water and in a canal. The result agrees qualitatively with experimental data (see Fig. 35). There are also many experimental results in this field. Bindel [124] and Helm [146] have obtained a critical speed range above which squat will cause a ship to touch the bottom (see Fig. 36).
Honda and others [145] have conducted extensive full scale measurements on squat at Malacca Strait and

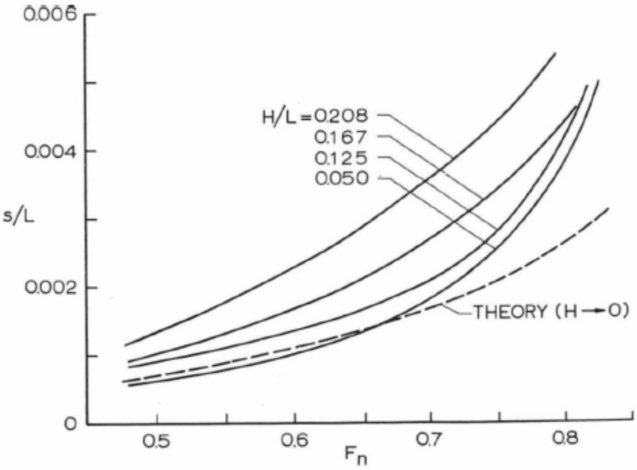

Fig. 35

compared the results with model experiment data. Experiments in restricted waters have been mostly conducted in towing tanks installed with false bottoms. However, it has been pointed out that experimental data conducted with false bottoms may include significant errors [144]. With this in mind, some establishments have begun to construct shallow water basins for this purpose. The new current and wave basin in NSMB is famous among this kind of basin [149].

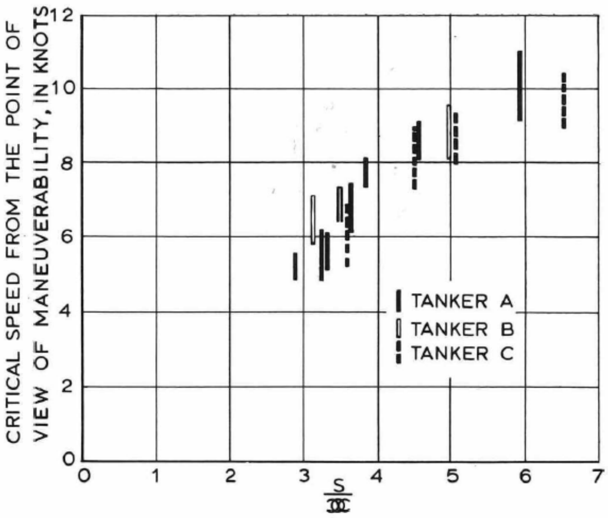

Fig. 36

Stopping maneuver

It is well known that in an emergency, the best method of avoiding a collision is to steer to hard over, provided there is enough sea room. This is because, except at low forward speeds, the forward distance travelled in a full turn is much smaller than that travelled after a full astern order is given. This relation is shown in Fig. 37. Nevertheless, the stopping maneuver is an important means of avoiding a collision since there may not be enough sea room to make a turn.

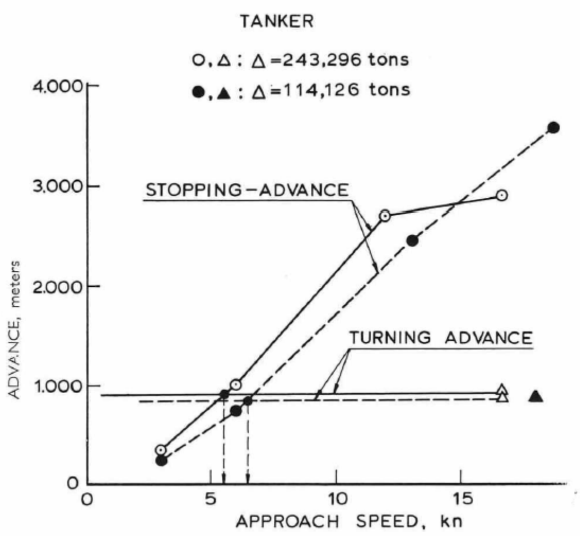

Fig. 37

Stopping distance

Since the speed of a ship stays almost constant as the size of the ship increases, the thrust of propeller per unit displacement of a ship decreases as the size of the ship increases. Therefore the stopping distance of ships has been increasing as the ship size has kept increasing. Fig. 38 shows the relation between the stopping distance and the displacement. Several trials, both theoretical and experi-

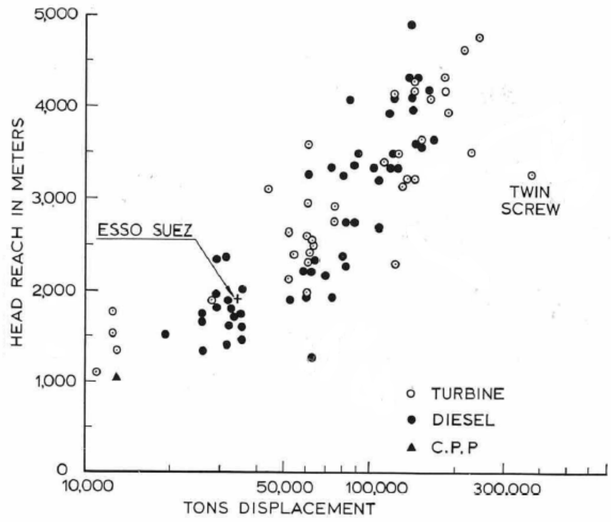

Fig. 38 Relation between stopping distance and displacement.

mental, to estimate the stopping distance have been made [156, 157, 158, 159, 160, 161, 162]. Among them, the work by Hewins, Chase and Ruiz [156, 157] and the further work by SNAME [160] are famous. According to [12], the fundamental equation of motion is written as:

$$(m + m_x)\frac{du}{dt} = T_p(1 - t_p) - R_h \qquad (25)$$

where T_p is the propeller thrust, t_p is the thrust deduction and R_h is the resistance of a ship. A change in the thrust can be separated into the following three groups;

a From the execution of a full astern order until the propeller thrust becomes zero. The propeller keeps turning in the right direction.

b From the generation of negative thrust until the propeller stops.

c From the beginning of the reverse turn of the propeller until the ship stops.

Assuming the thrust for these three stages [163, 162] eq. 25 can be solved, the stopping distance and time will be

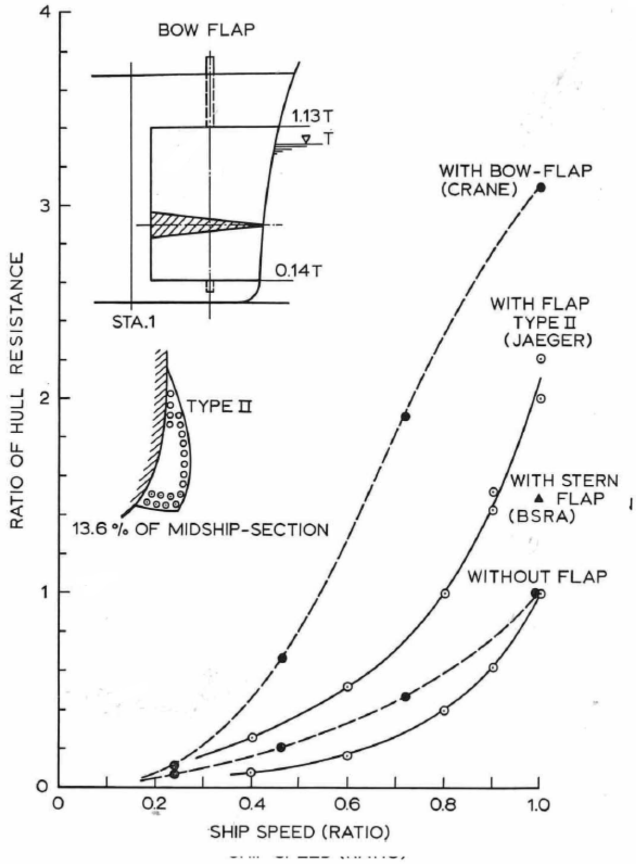

Fig. 39

obtained. In [12], a simplified method to obtain the stopping distance as function of the initial speed, initial resistance, and reverse thrust is shown. The effect of parameters such as the initial speed, type of propeller, type of engines etc. on the stopping distance has also been treated by many research workers [164, 165, 166, 169].

Effect of steering

The effect of steering during the stopping procedure is also an important and difficult problem. Hooft [167] measured the hydrodynamic force and moment acting on a stopping steered ship by the PMM technique, and Yamanouchi and others [168] conducted the same kind of measurements on a straight towed model. Both tests showed that the rudder force decreases drastically when the propeller is reversed resulting in a sudden loss of maneuverability. Tani [163], showed that the stopping distance is affected by the turning of the ship.

Auxiliary devices for emergency stops

To decrease the stopping distance particularly of large ships, several auxiliary methods have been tried.

1 Brake flaps
A bow flap [170, 189], a flap at the shoulder [171] and a stern flap [172] have all been tried, and a trial of opening up the rudder [173] has also been made. The ratio of hull resistances for each device is shown in Fig. 39. There is no doubt that these devices are effective to some extent, but there appear to be difficulties in the strength of the flaps.

2 Water parachutes
A full scale trial on a 80,000 DWT tanker installed with 4 parachutes has been made [174] in which parachutes were installed on board the deck and were dropped into water with ropes. It was reported that the stopping distance was decreased by 37%.

List of symbols

1 *Inertia*

m	mass
m_x, m_y, m_z	added mass for x, y, z direction
I_x, I_y, I_z	moment of inertia about x, y, z axis
J_x, J_y, J_z	added moment of inertia about x, y, z axis
α_x	distance between center of gravity (CG) and center of lateral added mass.

2 *Motions*

U	speed of CG.
u, v, w	x, y, z components of the speed
β	drift angle
δ	rudder angle
ψ	heading angle
$r=\dot{\psi}$	turning rate
$Fn=U/\sqrt{gL}$	Froude number
ω	circular frequency
t	time
ρ	density
g	acceleration of gravity
D	turning diameter
R	turning radius

3 *Force and moment*

X, Y, Z	x, y, z components of the force
N	moment about Z axis
X_u etc.	$\partial x/\partial u$ etc.
x_{uu} etc.	$\partial^2 x/\partial u^2$ etc., x_{uuu} etc., $\partial^3 x/\partial u^3$ etc.

4 *Non-dimensional expressions*

$m', m'_{x,y,z} = m, m_{x,y,z} / \frac{\rho}{2} L^3$

$I'_{x,y,z} = I_{x,y,z} / \frac{\rho}{2} L^5$

$J'_{x,y,z} = J_{x,y,z} / \frac{\rho}{2} L^5$

$t' = tU/L$

$u', v', w' = u, v, w/U$

$r' = rL/U$

$X', Y', Z' = X, Y, Z / \frac{\rho}{2} L^2 U^2$

$N' = N / \frac{\rho}{2} L^3 U^2$

$X'_{u,v,w} = X_{u,v,w} / \frac{\rho}{2} L^2 U$

$Y'_{u,v,w} = Y_{u,v,w} / \frac{\rho}{2} L^2 U$

$N'_{u,v,w} = N_{u,v,w} / \frac{\rho}{2} L^3 U$

$X'_r = X_r / \frac{\rho}{2} L^3 U$

$Y'_r = Y_r / \frac{\rho}{2} L^3 U$

$N'_r = N_r / \frac{\rho}{2} L^4 U$

$X'_{\dot{u},\dot{v},\dot{w}} = X_{\dot{u},\dot{v},\dot{w}} / \frac{\rho}{2} L^3$

$Y'_{\dot{u},\dot{v},\dot{w}} = Y_{\dot{u},\dot{v},\dot{w}} / \frac{\rho}{2} L^3$

$N'_{\dot{u},\dot{v},\dot{w}} = N_{\dot{u},\dot{v},\dot{w}} / \frac{\rho}{2} L^4$

$X'_{\dot{r}} = X_{\dot{r}} / \frac{\rho}{2} L^4$

$Y'_{\dot{r}} = Y_{\dot{r}} / \frac{\rho}{2} L^4$

$N'_{\dot{r}} = N_{\dot{r}} / \frac{\rho}{2} L^5$

$X'_\delta, Y'_\delta = X_\delta, Y_\delta / \frac{\rho}{2} L^2 U^2$

$N'_\delta = N_\delta / \frac{\rho}{2} L^3 U^2$

$X'_{uu}, Y'_{uu}, Z'_{uu} = X_{uu}, Y_{uu}, Z_{uu} / \frac{\rho}{2} L^2$

$X'_{uuu}, Y'_{uuu} = X_{uuu}, Y_{uuu} / \frac{\rho}{2} \frac{L^2}{U}$

Abbreviations

RINA	Royal Institute of Naval Architects
SNAME	Society of Naval Architects and Marine Engineers
NSRDC	Naval Ship Research and Development Center (former DTMB)
HyA	Hydro-og-Laboratorium
TH Delft	Technological University Delft
NSMB	Netherlands Ship Model Basin
SSPA	Swedish State Shipbuilding Experimental Tank
ISP	International Shipbuilding Progress
JSG	Jahrbuch der Schiffbautechnische Gesellschaft
JSNA Japan	Journal of the Society of Naval Architects of Japan
JSNA west Japan	Journal of the Society of Naval Architects of West Japan

References

1 W. Hovgaard. Turning Circles. TINA, 1912.

2 G. Weinblum & H. Künzel. Über die Kursstabilität von Schiffen. Schiffbau, 1938.

3 K. S. M. Davidson. Turning and Steering of Ships. SNAME, 1944.

4 K. S. M. Davidson & L. I. Schiff. Turning and Course-Keeping Qualities of Ships. SNAME, 1946.

5 G. Kempf. Maneuvering Standards of Ships. Deutsche Schiffahrts-Zeitschrifft, Hansa No. 27/28, 1944.

6 J. Dieudonné. Note sur la Stabilité du Régime de Route des Navires. Association Technique Maritime et Aeronautique, Session 1949.

7a K. Nomoto, K. Taguchi, K. Honda & S. Hirano. On the Steering Qualities of Ships (1). JSNA Japan, Vol. 99, 1956.

7b K. Nomoto & K. Taguchi. On the Steering Qualities of Ships (2). JSNA Japan, Vol. 101, pp. 57–66, Aug., (1957) (in Japanese).

8 K. Nomoto. On the Steering Qualities of Ships. ISP Vol. 4, 1957.

9 K. Nomoto. Analysis of Kempf's Standard Test. Proceedings of First Symposium on Ship Maneuverability, Washington 1960, DTMB Report 1461.

10 M. Gertler. Experimental Techniques Methods of Analysis Used in Submerged Body Search. Third Symposium on Naval Hydrodynamic, Scheveningen, The Netherlands, Sept. 1960.

11 M. Gertler. The DTMB Planar-Motion-Mechanism System. Symposium of Towing Tank Facilities, Zagreb, Yugoslavia, Sept. 1959.

12 N. H. Norrbin. A study of Course Keeping and Manoeuvring Performance. 1st Symp. On Ship Maneuverability, 1960.

13 S. Motora. On the Virtual Forces acting on a maneuvering Ship, and Initial Stage of Steered Motion. JSNA Japan, Vol. 95, 1954.

14 S. Motora. On the Course Stability of Ships. JSNA Japan, Vol. 77 1955 (read in 1946).

15 Sir H. Lamb. Hydrodynamics, 6th Edition.

16 M. Abkowitz. Lectures in Ship Hydrodynamics, Steering and Maneuverability. Hydro-Og Aerodynamisk Laboratorium, Report Hy-5, Lyngby, Copenhagen, Denmark, May 1964.

17 K. Nomoto. Approximate Nonlinear Analysis on Steering Motion. Formal contribution to the 12th ITTC, Rome, 1969.
18 G. van Leeuwen. A simplified Non-linear Model of a Manoeuvring Ship. TH Delft, Report 262, 1970.
19 N. H. Norrbin. On the Reduced Non-linear Equation of Steering and its Application to the Analysis of the Pullout Maneuver. Formal contribution to the 12th ITTC, Rome 1969.
20 C. C. Glansdorp. Simulation of Full-Scale Results of Manoeuvring Trials of a 200,000 tons Tanker with a simple Mathematical Model. THD Report, 1971.
21 M. Bech & L. W. Smitt. Analogue Simulation of Ship Maneuvers based on full-scale trials or free-sailing model tests. HyA Report Hy-14, 1969.
22 J. Strøm-Tejsen. A Digital Computer Technique for the Prediction of Standard Maneuvers of Surface Ships. DTMB Report 2130, Dec. 1965.
23 H. Eda & C. L. Crane Jr. Steering Characteristics of Ships in Calm Water and in Waves. Trans. SNAME, 1965.
24 D. Clarke. A New Non-linear Equation for Ship Manoeuvring. ISP Vol. 18, 1971.
25 O. Grim. Die Hydrodynamischen Kräft beim Rollversuch. Schiffstechnik Bd 3, 1955/56.
26 K. Tamura. The Calculation of Hydrodynamic Forces and Moments acting on the two-dimensional Body. JSNA West Japan, Vol. 21, 1963.
27 F. Tasai. Hydrodynamic Force and Moment Produced by Swaying and Rolling Oscillations of Cylinders on the Free Surface. Report of Institute of Applied Mechanics Univ. of Kyushu, Vol. IX, No. 35, 1961.
28 W. R. Porter. Added Mass, Damping and Wave-Ratio Coefficients for Swaying Ship-Like Cylinders. Journal of Ship Research.
29 E. O. Tuck. A New Approach to the Strip Theory of Forced Ship Motion. NSRDC Tech. Note, Sept. 1966.
30 G. van Leeuwen. The Lateral Damping and Added Mass of an Oscillating Ship model. Shipbuilding Laboratory, Delft, Publ. No. 23, July 1964.
31 N. H. Norrbin. Theory and Observations on the Use of a Mathematical Model for Ship Manoeuvring in Deep and Confined Waters. SSPA Report 68, 1971.
32 S. Motora & M. Fujino et al. Equivalent Added Mass of Ships in a Collision. JSNA Japan, Vol. 126, Dec. 1969.
33 S. Motora. On the Measurement of Added Mass and Added Moment of Inertia of Ships in Steering Motion. Proceedings of First Symposium on Ship Maneuverability, Washington 1960, DTMB Report 1461, 1960.
34 R. Brard. A Vortex Theory for the Manoeuvring Ship with respect to the History of her Motion. 5th Symposium on Naval Hydrodynamics, Bergen 1964.
35 J. N. Newman. Some Hydrodynamic Aspects of Ship Maneuverability. 6th Symposium on Naval Hydrodynamics, Washington D.C., 1966.
36 M. Gertler. Report of the Manoeuvrability Committee 12th ITTC Rome, 1969 Appendix 3, Part 2.
37 M. Gertler. Cooperative Rotating Arm and Straightline Experiments with ITTC Standard Model. DTMB Report 2221, 1966.
38 M. S. Chislett & J. Strøm-Tejsen. Planar Motion Mechanism Tests and Full Scale Steering and Full-Scale Steering Maneuvering Predictions for a Mariner Class Vessel. Hydro- Og Aerodynamisk Laboratorium, Report HyA 6, Lyngby, Denmark, April 1965.
39 J. R. Paulling & O. I. Sibul. New Experiment and Techniques for the Experimental Evaluation of Ship's Lateral Stability. Univ. of California Inst. of Engineering Research Report, August, 1962.
40 G. van Leeuwen & C. C. Glansdorp. Experimental Determination of Linear and Non-linear Hydrodynamic Derivatives of a Mariner-Type Ship Model. TH Delft Report No. 145, 1966. Also Formal contribution to the 11th ITTC, Tokyo, 1966.
40′ S. Motora & M. Fujino. On the Measurement of Stability Derivatives of Mariner Type Ship by Forced Yawing Technique. Formal contribution to the 11th ITTC, Tokyo, 1966.
41 G. A. Firsoff. Hydrodynamic Characteristics of a Ship Model of the Mariner Type. Written contribution to 11th ITTC, Tokyo, 1966.
42 A. Suarez. Rotating Arm Experimental Study of a Mariner Class Vessel. Davidson Laboratory Note 696, June 1963.
43 R. K. Burcher. Co-operative Tests for ITTC Mariner Class Ship Rotating Arm Experiments. Formal contribution to the 12th ITTC, Rome, 1969.
44 H. Kasai. Forced Oscillation Test on a 6 m Mariner Model. Formal contribution to the 11th ITTC, Tokyo, 1966.
45 R. V. Morse & D. Price. Maneuvering Characteristics of the Mariner Class Ship in Calm Seas. Sperry Gyroscope Company Report GJ-2233-1019, Dec. 1961.
46 Principles of Naval Architecture (New edition, SNAME 1967).
47 W. Bolley. A Non-linear Wing Theory and its Application to Rectangular wings of Small Aspect Ratio. ZAMM, 19. Bd, Nr. 1, Febr. 1939.
48 R. T. Jones. Properties of Low Aspect Ratio Pointed Wing at Speeds Below and Above the Speed of Sound. NACA Rep. No. 835, 1946.
49 H. R. Lawrence. The Lift Distribution on Low Aspect Ratio Wings at Subsonic Speed. Coronel Aeronautical Laboratory report No. AF-673-A-1, 1950.
50 H. Thieme. Über Strömungstechnische Grundlagen Zur Bestimmung von Steuereigenschaften. Schiff und Hafen, 1954.
51 W. R. Jacobs. Method of Predicting Course Stability and Turning Qualities of Ships. Davidson Laboratory Report 945, March 1963.
52 S. Inoue. On the Turning of Ships. Memoirs of the Faculty of Engineering, Kyushu University, 1956.

53 K. K. Fedyaevsky & G. V. Sobolev. Application of the Results of low Aspects Ratio Wing Theory to the Solution of Some Steering Problems. Symposium on the behaviour of ships in a seaway, Wageningen, 1957.
54 N. H. Norrbin. Forces in Oblique Towing of a Model of Cargo Liner and a Divided Double-Body Geosim. SSPA Pub. No. 57.
55 J. N. Newman. Some Hydrodynamic Aspects of Ship Maneuverability. 7th Symposium on Naval Hydrodynamics, Washington D.C., 1966.
56 H. Fisher. Berechnung der Rudeskraft. W.R.H., 1938.
57 G. H. Bottomley. Manoeuvring of Ships, Part II–IV. Institute of Shipbuilders and Enginebuilders in Scotland, 1923–31.
58 S. Akazaki. On the normal force and its center of rudders, Part 1–4. JSNA Japan, Vol. 63, 67, 68, 69, 1937–41.
59 A. Suarez. The Davidson Laboratory Rotating-Arm Facility. Davidson Laboratory Note 597, June 1960.
60 R. C. Darnell. Hydrodynamic characteristics of twelve symmetrical Hydrofoils. DTMB Report 341.
61 P. Mandel. Some Hydrodynamic Aspects of Appendage Design. Trans. SNAME 1953.
62 S. Okada. On the performance of rudders behind the ship body, Part 1–5. JSNA Japan Vol. 103–105, 1959.
63 A. Fujii and T. Tsuda. On the study of Rudder Performance by Free-running Models. JSNA Japan, Vol. 110, 1961.
64 M. Bech. The Reversed Spiral Test as Applied to Large Ships. Shipping World, Nov., 1968.
65 L. W. Smitt. The Reversed Spiral Test-a Note on Bech's Spiral Test and some Unexpected Results of its Application to Coasters. HyA Report Hy-10, May 1967.
66 S. Motora & M. Fujino. On the Modified Zig-zag Maneuver test. JSNA Japan, Vol. 128, 1970, Also Formal contribution to the 12th ITTC Rome, 1969.
67 R. K. Burcher. Status Report on Pull out and Weave Maneuvers. Admiralty Experiment Works, Haslar P0122 AG, 1969.
68 K. Karasuno. Full scale Measurement of Steering Transfer Function. Full scale parallel shift maneuver. JSNA Vol. 128, 1970.
69 R. I. Price. Maneuvering Data, IMCO Maritime Safety Committee Recommendation. Marine Technology, Vol. 7, No. 3, 1970.
70 H. Thieme. Manövrier- und Ruderversuche METEOR. Beitrag zur Frage des Massstabseffektes. IfS Report 239, 1968.
71 G. A. Firsoff. The New Tank for Studying the Manoeuvrability of Ships. Formal contribution to the 12th ITTC, Rome, 1969.
72 L. W. Smitt & M. S. Chislett. A Brief Discription of HyA Large Amplitude PMM System. IUTAM Conference, London, 1972.
73 S. Motora & M. Fujino. On the New Sea Keeping Basin of the University of Tokyo. Formal contribution to the 12th ITTC, Rome, 1969.
74a A. Suarez. Appendix 1 of the Maneuverability Committee Report, 11th ITTC, Tokyo, 1966.
74b A. Suarez. First Analysis Phase of the Free Model Maneuvering Tests. Appendix 3, Part 1. Maneuverability Committee 12th ITTC, Rome, 1969.
75 K. Nomoto. Analysis of the ITTC Maneuverability Tests for the Mariner Type Ship in Terms of Steering Quality Indices K and T. 11th ITTC, Tokyo, 1966.
76 A. J. Vosper. Correlation between Model Tests and Ship Trials Data. Appendix 4, Manoeuvrability Committee Report, 12th ITTC, Rome, 1969.
77 U. Niemann. Der Einfluss der Zähigkeit auf QuerKräfte und Momente an Manövrierenden Schiffen. JSG Vol. 61, 1967.
78 H. Fujii. Investigations into the Rudder Performance by a Free Running Model (1). JSNA Japan, Vol. 107, 1960.
79 S. Motora & M. Fujino. On the Measurement of the Stability Derivatives by means of Forced Yawing Technique. JSNA Japan, Vol. 118, 1965.
80 K. Kawano et al. On the Model-Ship Correlation in Maneuverability Experiments. JSNA Japan, Vol. 107, 1960.
81 H. Thieme. Appendix 3 of the Maneuverability Committee Report, 11th ITTC Tokyo, 1966.
82 H. Thieme. Appendix 4 of the Maneuverability Committee Report, 12th ITTC Rome, 1969.
83 M. Rakamarić & J. Korlević. On the Possibility to Simulate higher Reynolds Number Condition for Rudder model by Increasing its Surface Temperature. Formal contribution to the 12th ITTC, Rome, 1969.
84 K. Nomoto. Unusual Scale Effect on Maneuverabilities of Ships With Blunt Bodies. Formal Contribution to the 11th ITTC, Tokyo, 1966.
85 H. Fujii. Experimental Techniques on the Maneuverability. 2nd Symposium on Maneuverability, JSNA, Nov. 1970.
86 S. Motora, M. Takagi, A. Kokumai, H. Kato, & T. Koyama. An analysis of the Maneuverabilty of Ships Associated with Unusual characteristics under Steerage. JSNA Japan, Vol. 128, 1970.
87 A. Vosper. A Note Ship-Model Correlation. AEW, 1967.
88 M. Gertler & S. C. Gover. Handling Quality Criteria for Surface Ships. Chesapeake Section, SNAME, 1959.
89 L. Segel. Ship Maneuverability as Influenced by Transient Response to the Helm. DTMB Report 1461, Oct. 1960.
90 K. Nomoto and N. H. Norrbin. Appendix 1 of the Maneuverability Committee Report, 12th ITTC, Rome, 1968.
91 N. Norrbin. On the Design and Analysis of the Zig-zag Test on Base of Quasi-Linear Frequency Response. SSPA Report No. B 104-3, Formal contribution to 10th ITTC, London, 1963.
92 N. Norrbin. Zig-zag Test Technique and Analysis with Preliminary Statistical Results. SSPA Report No. 12, June 1965 (in Swedish), also BSRA translation No. 2188.
93 J. B. van den Brug & W. A. Wagenaar. An Experimental Simulator for the Manoeuvring of Surface Ships. ISP Vol. 16, No. 180, 1969.

94 J. D. van Manen, J. B. van den Brug, W. A. Wagenaar & C. Don. The Netherlands Ship Model Basin Ship Handling and Manoeuvring Simulator. ISP Vol. 17, No. 185, 1970.
95 A. Ogawa. Manoeuvrability of Ships under Influence of External Forces (Part I). JSNA Japan Vol. 126, 1969.
96 N. H. Norrbin. Theory and Observation on the Use of Mathematical Model for Ship Manoeuvring in Deep and Confined Waters. SSPA No. 68, 1971.
97 S. Inoue, M. Murakami, M. Hirano and T. Inoue. On Turning Loci of Ships in calm Water. JSNA West Japan, Vol. 37, 1969.
98 H. Eda & C. L. Crane Jr. Steering Characteristics of Ships in Calm Water and Waves. SNAME Vol. 73, 1965.
99 A. Sugisaki. Fundamental Concept of Automated Watching. Journal of The Navigation Society of Japan, 1969.
100 I. Watanabe. Simulation of Traffic in Narrow Strait. Graduation Thesis, Univ. of Tokyo, 1970.
101. W. Marks et al. An Automated System for Optimum Ship Routing. TSNSME Vol. 76, 1968.
102 T. Koyama. On an Optimum Control of a Ship in Rough Seas. JSNA Japan, Vol. 122, 1967.
103 S. Motora. On the Automatic Control and Yawing of a Ship in Rough Seas. JSNA Japan, Vol. 94, 1954.
104. L. J. Rydill. A Linear Theory of the Steered Motion of ships in Waves. TINA, Vol. 101, 1959.
105 P. Mandel. Subcritical and Supercritical Operation of Ships in Waves. JSR Vol. 4, 1960.
106 K. Nomoto & N. Motoyama. On Loss of SHP due to Yawing. JSNA Japan, Vol. 104, 1959.
107 S. Motora & T. Koyama. On an Improvement of Ship Manoeuvrability by means of Automatic Control. JSNA Japan, Vol. 116, 1964.
108 H. Tani. Analysis of Ship-steering Engine-helmsman system Chap. 5. 60th Anniversary Series SNA Japan, 1966.
109 A. M. Stuurman. Modelling the Helmsman. Formal contribution to the 12th ITTC, Rome, 1969.
110 J. P. Hooft. The Manoeuvrability of Ships on a Straight Course. ISP Vol. 15, No. 162, 1968.
111 J. K. Zuidweg. Automatic Guidance of Ships as a Control Problem. Doctoral Thesis TH Delft, 1970.
112 G. J. Olsder. On the Time Optimal Bang-Bang Control of Linear Multivariable Systems with Small Initial Perturbations. Doctoral Thesis, Univ. of Groningen, 1971.
113 T. Tagori & A. Tanaka. Manoeuvring tests in a Circulation Tank and an Experiment on Automatic Tracking of Route. JSNA Japan, Vol. 126, 1969.
114a G. S. Baker. The Steering of Ships in Shallow Water and Canals. TINA, Vol. 66, 1924.
114b G. S. Baker. The Effect of Shallow Water on the Movement of a Ship. TINA, Vol. 94, 1952.
115 H. Schmidt-Stiebitz. Einfluß der Hauptspantform auf der Drehkreis von Flachwasserschiffen. Schiffstechnik, Heft 28, 1958.
116 H. Schmidt-Stiebitz. Untersuchungen über den Einfluß der Hauptspantform auf das Drehkreisverhalten von Flachwasserschiffen. Teil II: Schrägschleppfahrten. Schiffstechnik, Heft 32, 1959.
117 H. Schmidt-Stiebitz. Einfluß des Wellenbildes auf das Drehkreisverhalten von Flachwasserschiffen bei größeren Geschwindigkeiten. Forschungsberichte des Landes Nordrhein-Westfalen, Nr. 774. 23. Veröffentlichung der VBD, 1959.
118 H. Schmidt-Stiebitz. Ein experimenteller Beitrag zu Drehkreismanövern von Schiffen auf flachem und tiefem Wasser. Schiff und Hafen, H. 11, H. 12, 1963; H. 11, 1964.
119 H. Schmidt-Stiebitz. Die Manövrier-Eigenschaften der Schiffe im Abhängigkeit von Schiffsform und Fahrwasser. Schiff und Hafen. H. 2. 1964.
120 R. S. Garthune, B. Rosenberg, D. Cafiero, and C. R. Olson. The Performance of Model Ships in Restricted Channels in Relation to the Design of a Ship Canal. DTMB Report 601, Aug. 1948.
121 C. G. Moody. The Handling of Live Super Ships through Gaillard Cut of the Panama Canal. DTMB Report 1277, Oct. 1958.
122 C. G. Moody. The Handling of Ships through a Widened and Asymmetrically Deepened Section of Gaillard Cut in the Panama Canal. DTMB Report 1705, Aug. 1964.
123 R. Brard. Manoeuvring of Ships in Deep Water, in Shallow Water, and in Canals. TSNAME, 1951.
124 S. Bindel. Experiments on Ship Manoeuvrability in Canals as Carried out in the Paris Model Basin. Proc. DTMB Symp. on Ship Manoeuvrability, May 1960.
125 T. Constantine. On the movement of ships in restricted water ways. Journal of fluid mechanics, Vol. 9, 1960.
126 S. Motora & M. Fujino. Appendix 4, Report of the Manoeuvrability Committee, 11th ITTC, Tokyo, 1966.
127 N. H. Norrbin. Part 1 and 3, Appendix 2, Report of the Manoeuvrability Committee, 12th ITTC, Rome, 1969.
128 S. Motora. Part 2, Appendix 4, Report of the Manoeuvrability Committee, 12th ITTC, Rome, 1969.
129 M. Fujino. Experimental Studies on Ship Manoeuvrability in Restricted Waters, Part 1. ISP Vol. 15, No. 168, Aug. 1968.
130 M. Fujino. Experimental Studies on Ship Manoeuvrability in Restricted Waters, Part 2. ISP Vol. 17, No. 186, Feb. 1970.
131 M. Kan and T. Hanaoka. Analysis of the Effect of Shallow Water upon Turning. JSNA Japan, Vol. 115, June, 1964.
132 J. N. Newman. Lateral motion of a slender body between two parallel walls. Journal of Fluid Mechanics, Vol. 39, 1969.
133 E. O. Tuck. Shallow water flows past slender bodies. Journal of Fluid Mechanics, 1966.
134 E. O. Tuck. Sinkage and trim in shallow water of finite width. Schiffstechnik, Bd. 14, 1967.

135 S. Inoue and K. Murayama. Calculation of Turning Ship Derivatives in Shallow Water. JSNA West Japan, No. 39, March 1970 (in Japanese).
136 S. Inoue and K. Kijima. Force Calculation of a Rectangular Plate Moving Obliquely in Water Channels. JSNA West Japan Vol. 39, 1970 (in Japanese).
137 S. Motora and R. B. Couch. Manoeuvrability of Full Bodied Ships in Restricted Waters. SNAME, Great Lakes and Great Rivers Section, Oct. 1961.
138 Report of SR 98 Ship Research Association of Japan, 1968, 1969.
139 N. Koseki and T. Tsuji. Shallow Water Effects upon Turning Ability. Report of the 1st Research Committee of Ship Research Institute, Nov. 1963.
140 N. Koseki, Y. Yamanouchi, S. Matsuoka and Y. Yamazaki. Some Model Experiments on Shallow Water Effects upon Turning Ability. JSNA Japan, Vol. 117, June, 1965.
141 K. E. Schoenherr. Data for estimating bank suction effects in restricted water on merchant ship hulls. First symposium on Ship Maneuverability, Washington, 1960, DTMB.
142 H. Eda & D. Savitsky. Experimental and Analytical Studies of Ship Controllability in Canals. Davidson Laboratory Techn. Note 809, Sept. 1969.
143 H. Eda. Directional Stability and Control of Ships in Restricted Channels. SNAME, 1971.
144 W. P. A. van Lammeren and J. D. van Manen. Correlation of Model and Ship Trials of a Shallow Draught Rhine Vessel. North East Coast Institution of Engineers and Shipbuilders, Vol. 70, 1953/54.
145 Report of the Ship Handling Laboratory, Kobe Univ. of Merchant Marine, No. I, II, III, 1964–66.
146 K. Helm und H. Heuser. Systematische Ruderversuche mit einem Schleppkahn und einem Binnenselbstfahrer vom Typ 'Gustav Koenigs' mit Kort-Düse. Schiff und Hafen, 12.7, 1960.
147 J. P. Hooft. On the Critical Speed Range of Ships in Restricted Waterways. ISP Vol. 16, No. 177, May 1969.
148 R. W. L. Gawn. Steering and Propulsion of H.M.S. Nelson in a Restricted Channel. TINA, Vol. 92, 1950 Ship Rec., Sept. 8, 1949.
149 W. P. A. van Lammeren and A. J. W. Lap. The combined wave and current Laboratory of the Netherlands Ship Model Basin. ISP Vol. 11, No. 118, June 1964.
150 G. Weinblum. Theoretische Untersuchungen der Strömungsbeeinflussung. Schiffbau, 15, Mar., 1933.
151 S. Schuster. Untersuchungen über Strömungs und Widerstandsverhältnisse bei der Fahrt von Schiffen in beschränktem Wasser. Jahrb. STG, 46. Bd.
152 B. L. Silverstein. Linearized Theory of the Interaction of Ships. Inst. Engng. Research, Report Series 82, Issue 3, Univ. of California, Berkeley 1957.
153 G. Weinblum. Wellenwiderstand auf beschränktem Wasser. Jahrb. STG, 39. Bd., 1938.
154 W. Graff. Untersuchungen über Anderungen von Sog und Nachstrom auf beschränkter Wassertiefe in stehendem und strömendem Wasser. Schiffstechnik, 8. Bd, Heft 44, Nov. 1961.
155 J. R. Paulling & L. W. Wood. The Dynamic Problem of Two Ships Operating on Parallel Courses in Close Proximity. University of California Series 189, July 1962.
156 E. F. Hewings, H. J. Chase & A. L. Ruiz. The Backing Power of Geared-Turbine-Driven Vessels. Transactions SNAME, Vol. 58, 1950, pp. 261–328.
157 H. J. Chase & A. L. Ruiz. A Theoretical Study of the Stopping of Ships. Transactions SNAME Vol. 58, 1950, pp. 811/854.
158 M. Kinoshita & Y. Nakajima. Motion, the Thrust and the Torque of Retarding Ships. JSNA Japan, Vol. 83, 1951.
159 Report of the Panel SR9. Shipbuilding Research Association of Japan 1956.
160 M9 Panel of the Ships Machinery Committee. Guide to the Selection of Backing Power. The Society of Naval Architects and Marine Engineers, Technical and Research Bulletin No. 3–5, 1957.
161 John C. Sainsbury. Stopping the Ship. Ship and Boat Builder, Dec. 1963, pp. 34–37.
162 J. Ritterhoff. Beitrag zur Erhöhung der Sicherheit von Schiffsantriebsanlagen durch Untersuchung ihres Manövrierverhaltens. Schiff und Hafen, Heft 3, 1970, s. 227–243.
163 H. Tani. On the stopping ability of ships. JSNA Japan, Vol. 120 1966.
164 Y. Watanabe. On the Calculation of Advance and Time in Stopping Maneuvers. JSNA Japan, Vol. 55, 1934.
165 S. M. Robinson. The Stopping of Ships. Journal of American Society of Naval Engineers, Vol. 50, No. 4, Nov. 1934, pp. 325–340.
166 J. P. Hooft. The Steering of a Ship during the Stopping Manoeuvre. Netherlands Ship Research Center, TNO. Report No. 114 S. Sept. 1969.
167 J. P. Hooft. The Maneuverability of Ships at Low Speed. TNO Report No. 138 S., 1970.
168 Y. Yamanouchi et al. On Model Experiments on the Manoeuvrability at Slow Speed and in Transient Conditions of a Patrol Ship. Report of Ship Research Institute, Vol. 1 No. 3, 1964.
169 J. P. Hooft & J. D. van Manen. The Effect of Propeller Type on the Stopping Ability of Ships. ISP, 1968.
170 C. L. Crane Jr. Methods to Improve Ship Stopping Performance. Stevens Institute of Technology, Davidson Laboratory, Report 1208, May 1967.
171 H. E. Jaeger et M. Jourdain. Le Freinage de Grands Navires (1). Bulletin de l'Association Technique Maritime et Aéronautique, No. 61, 1962, pp. 625–664.
172 D. Clarke & F. Wellman. Stopping Large Tankers and the Use of Auxiliary Braking Devices. Shipping World and Shipbuilder, May 1970, pp. 668–675.
173 E. Tasaka. The Braking of Ship by means of a Hinged Rudder. Scientific Asahi, Sept., 1964, pp. 104–107.

174a Progress in Marine Engineering in Japan, Japan Ship's Machinery Development Association, 1970.
174b Mitsubishi Shipbuilding News, No. 60, June, 1970.
175 Proceedings of the 1st Symposium on the Ship Maneuverability, SNA Japan, 1964.
176 Proceedings of the 2nd Symposium on the Ship Maneuverability, SNA Japan, 1970.
177 H. H. Chen. Some Aspects of Ship Maneuverability. Journ. Ship Research, Vol. 13, No. 2, 1969.
178 R. E. D. Bishop and A. G. Parkinson. On the Planar Motion Mechanism Used in Ship Model Testing. Phil. Soc. Trans., Series A, Vol. 266, 1970.
179 J. P. Hooft and I. Oldenkamp. Construction, Operation and Capabilities of the NSMB Ship Manoeuvring Simulator. Netherlands Ship Model Basin Publ. No. 382, 1971.
180 N. H. Norrbin and S. Göransson. The SSPA Steering and Manoeuvring Simulator. SSPA Allm. Rapport No. 28, 1969 (in Swedish).
181 A. McKenzie. Background and Information on the Marine Research and Training Center at Grenoble. 13th Annual Tanker Conf., Williamsburg, Virginia, 1968.
182 H. Eda. Steering Control of Ships in Waves. Davidson Laboratory Report DL-69-1205, 1967.
183 H. Eda. Low-Speed Controllability of Ships in Wind. Journ. Ship Research, Vol. 12, No. 3, 1968.
184 C. R. Kelley. A Predictor Instrument for Manual Control. Eighth Annual ONR Human Engineering Conf., Ann Arbor, Michigan, 1968.
185 W. B. van Berlekom. Predictor Systems for Safer Manoeuvring of Nuclear Ships into Ports. Paper presented at the Symposium on Nuclear Ships, Hamburg, 1971.
186 N. Norrbin. On Ship Maneuvering with Application to Shipborne Predictors and Real-Time Simulators. IUTAM Symposium, London, April 1972.
187 T. Koyama. Inprovement of Course Stability and Control by the Subsidiary Automatic Control. IUTAM Symposium, London, April, 1972.
188 M. I. Bech. Some Guidelines to the Optimum Adjustment of Auto Pilots in Ships. Paper presented at Symposium in Delft, 1970.
189 Technical University, Gdansk. Stopping and Auxiliary Device for Ships. 4th Subcommittee of Design and Equipment, IMCO, 1971.